Supplementary Information

Square Planar Mononuclear Ni(II) Complexes of Functionalized 2,2':6',2''-Terpyridines: BSA/DNA Binding and Anticancer Activity

Rakesh R Panicker, Martin Luther John, Daphne Morrison N, Pralayakaveri Yogendra Varma, Dharani S, Chayan Pandya, A. S. Vijai Anand, Joydip Mondal, Akella Sivaramakrishna*

Department of Chemistry, School of Advanced Sciences, Vellore Institute of Technology, Vellore 632014, Tamil Nadu, India

E-mail: asrkrishna@vit.ac.in

List of Figures

List of Tables

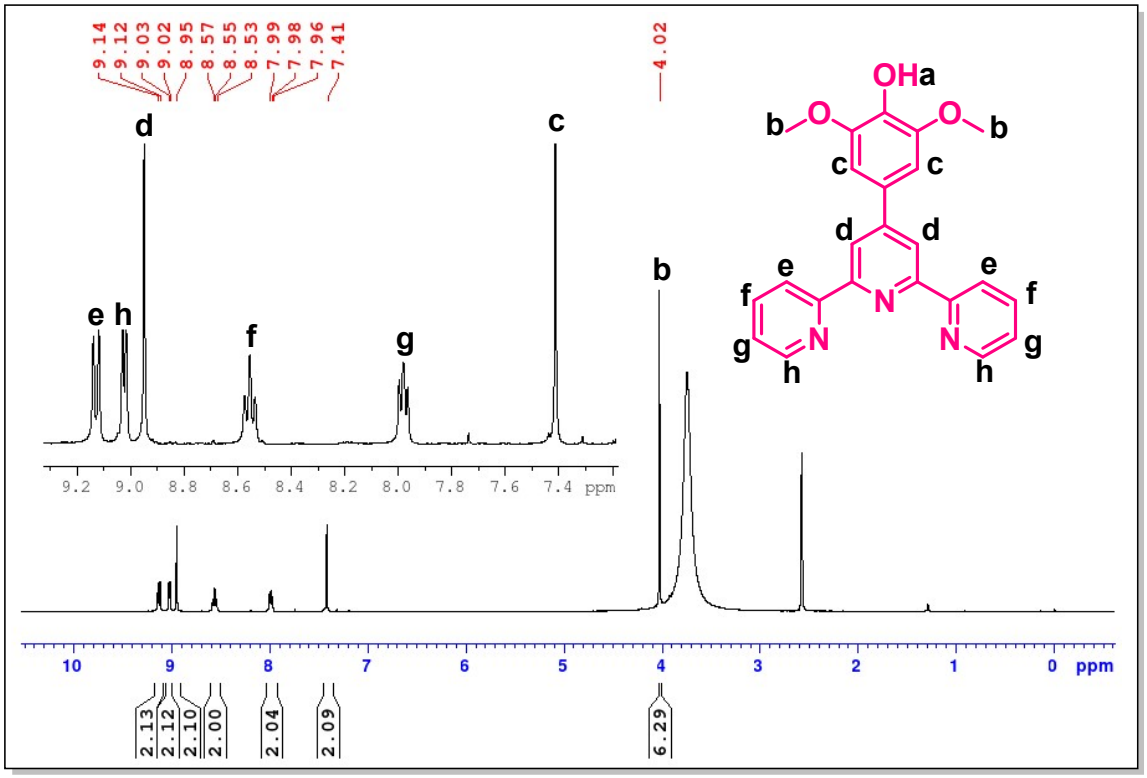

Figure S1. ^{1}H NMR Spectrum of compound **L1**

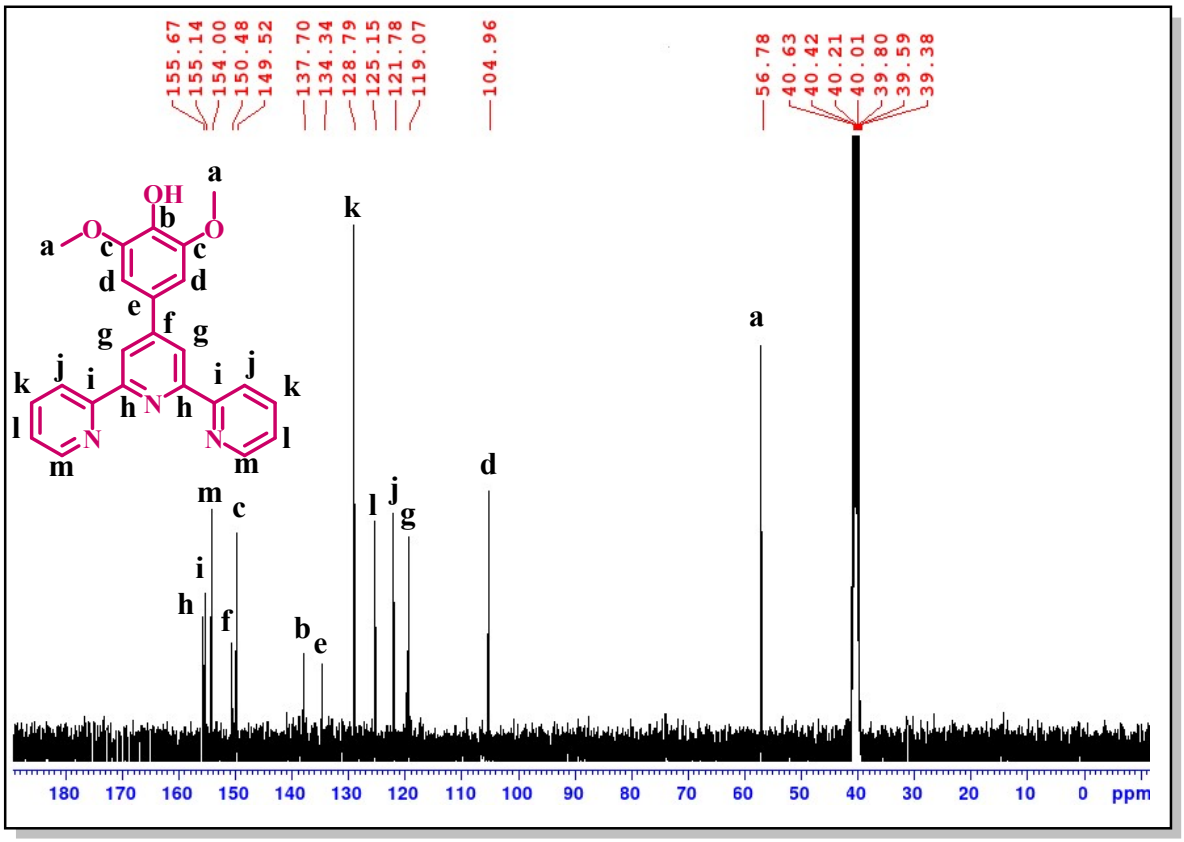

Figure S2. ^{13}C NMR Spectrum of compound **L1**

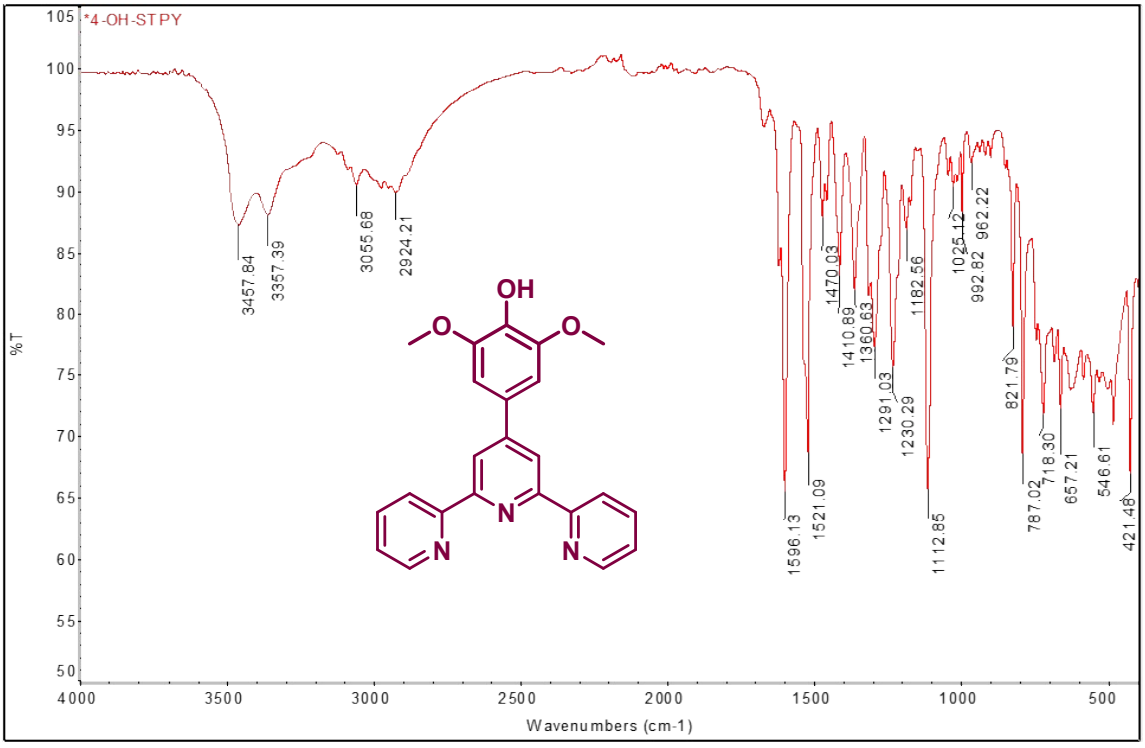

Figure S3. IR Spectrum of compound **L1**

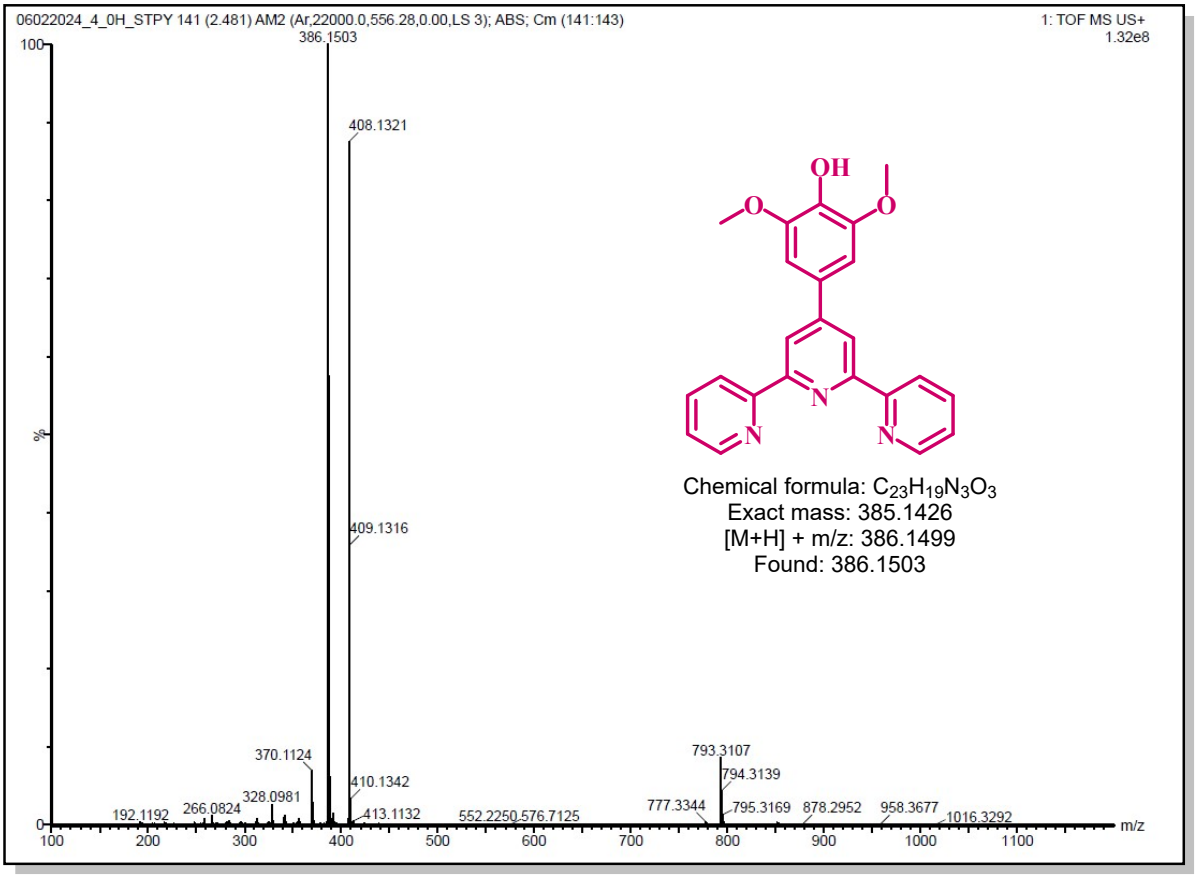

Figure S4. ESI-Mass Spectrum of compound **L1**

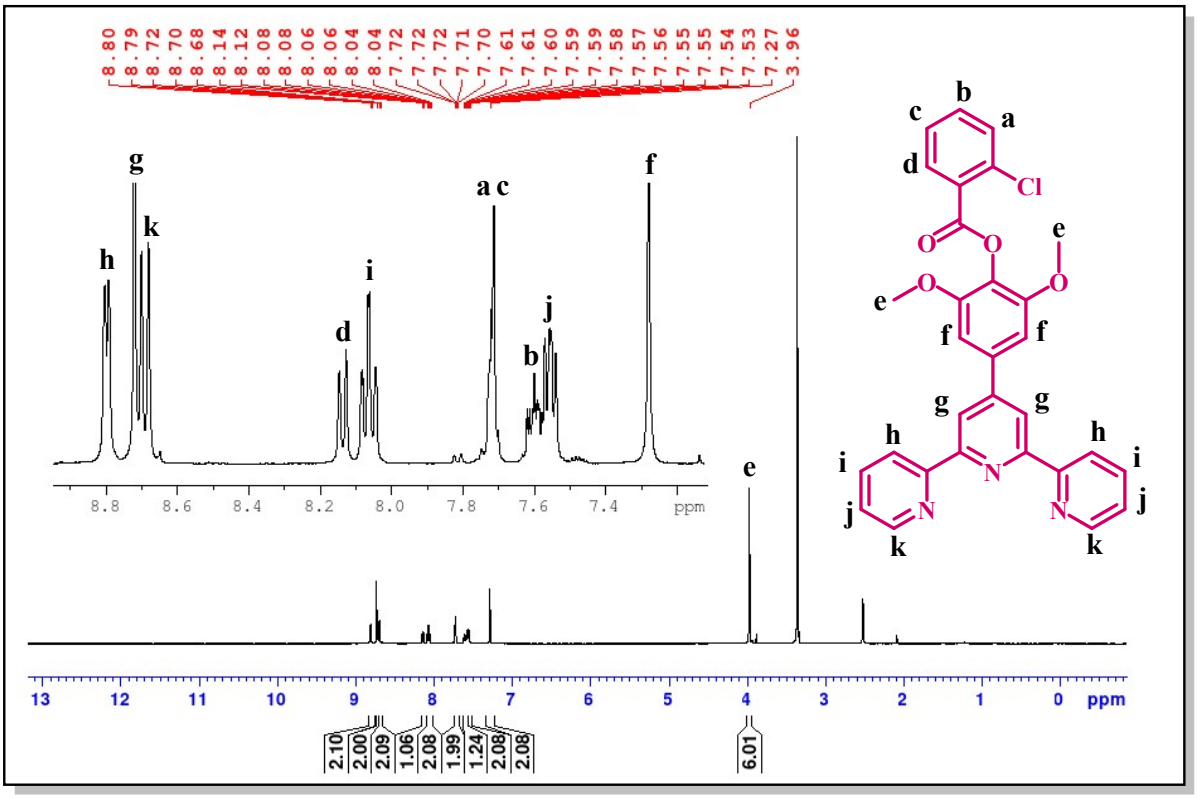

Figure S5. ^{1}H NMR Spectrum of compound **L2**

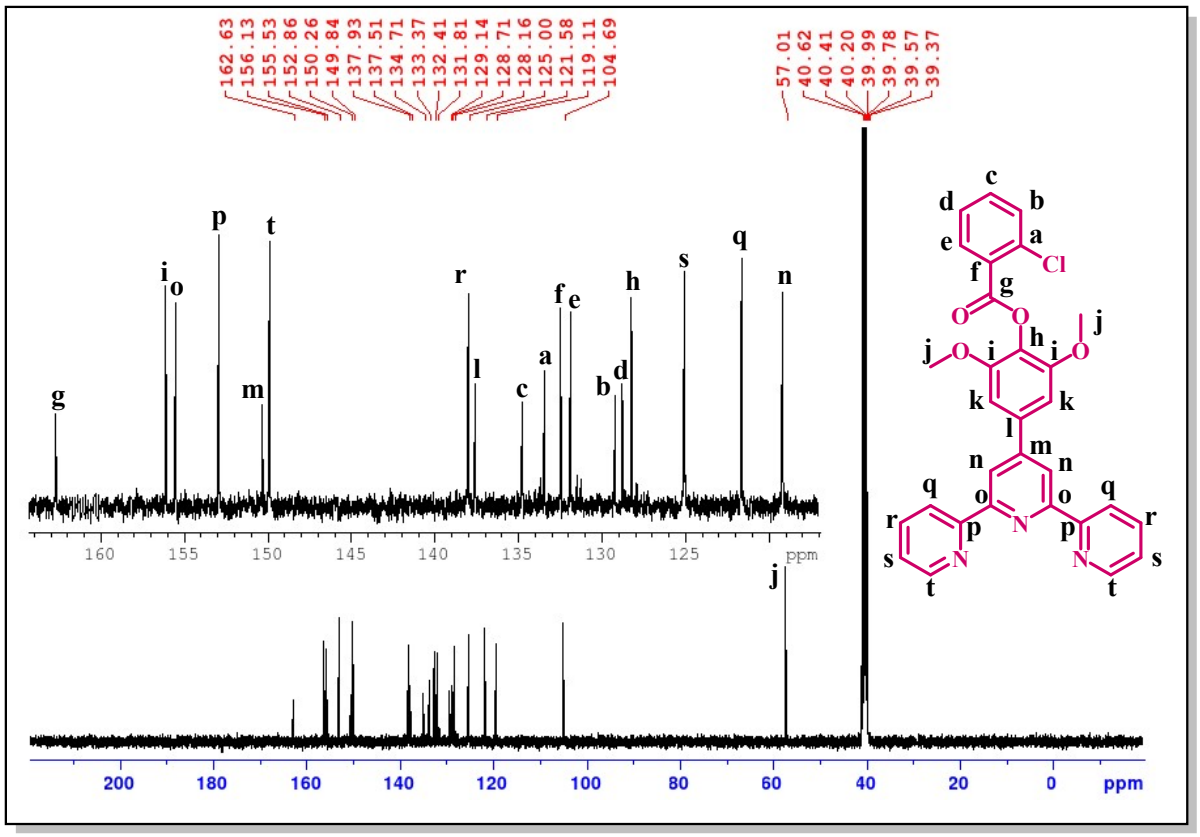

Figure S6. ^{13}C NMR Spectrum of compound **L2**

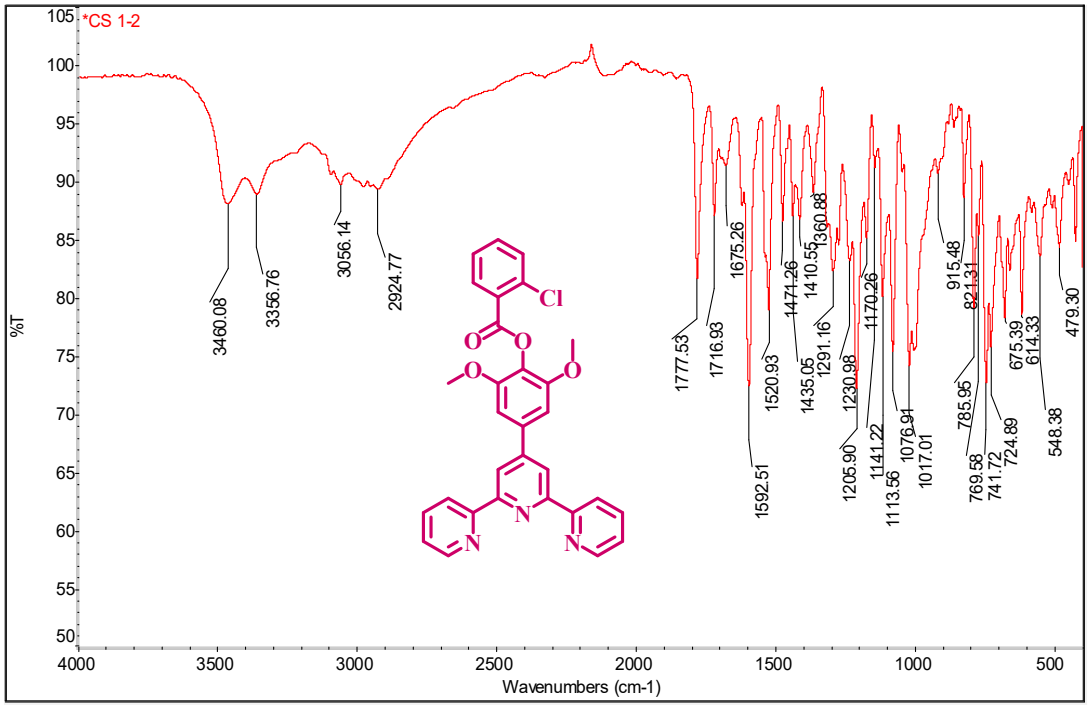

Figure S7. IR Spectrum of compound **L2**

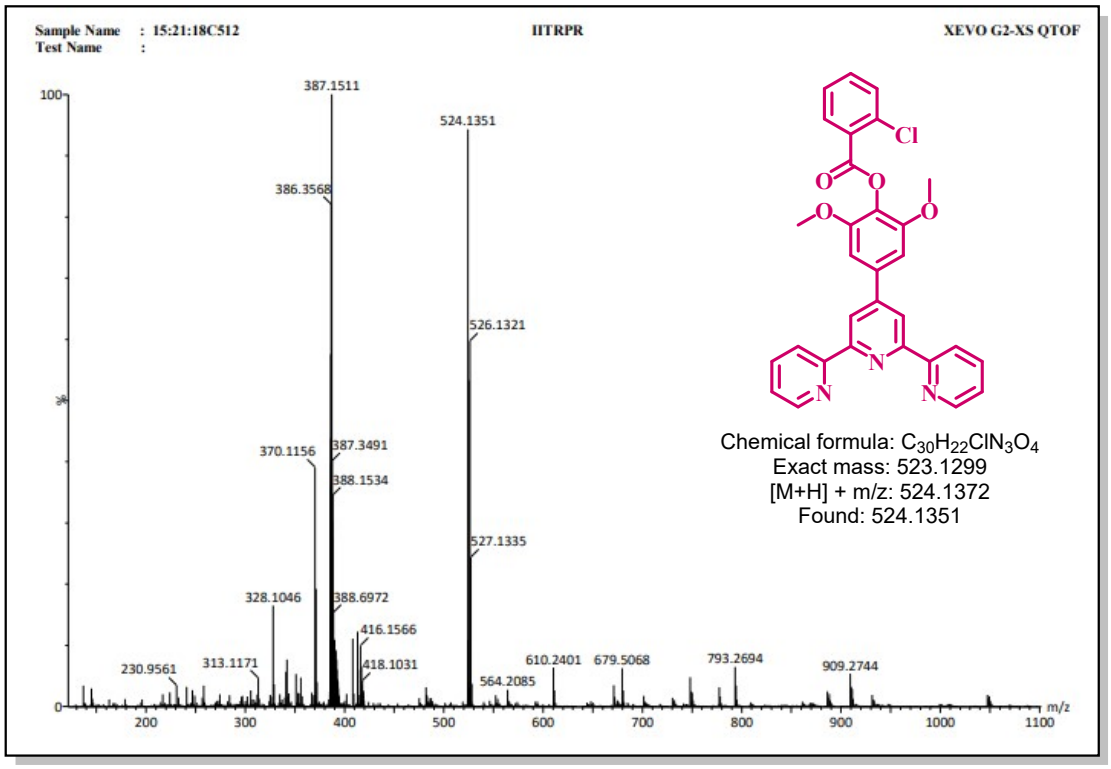

Figure S8. ESI-Mass Spectrum of compound **L2**

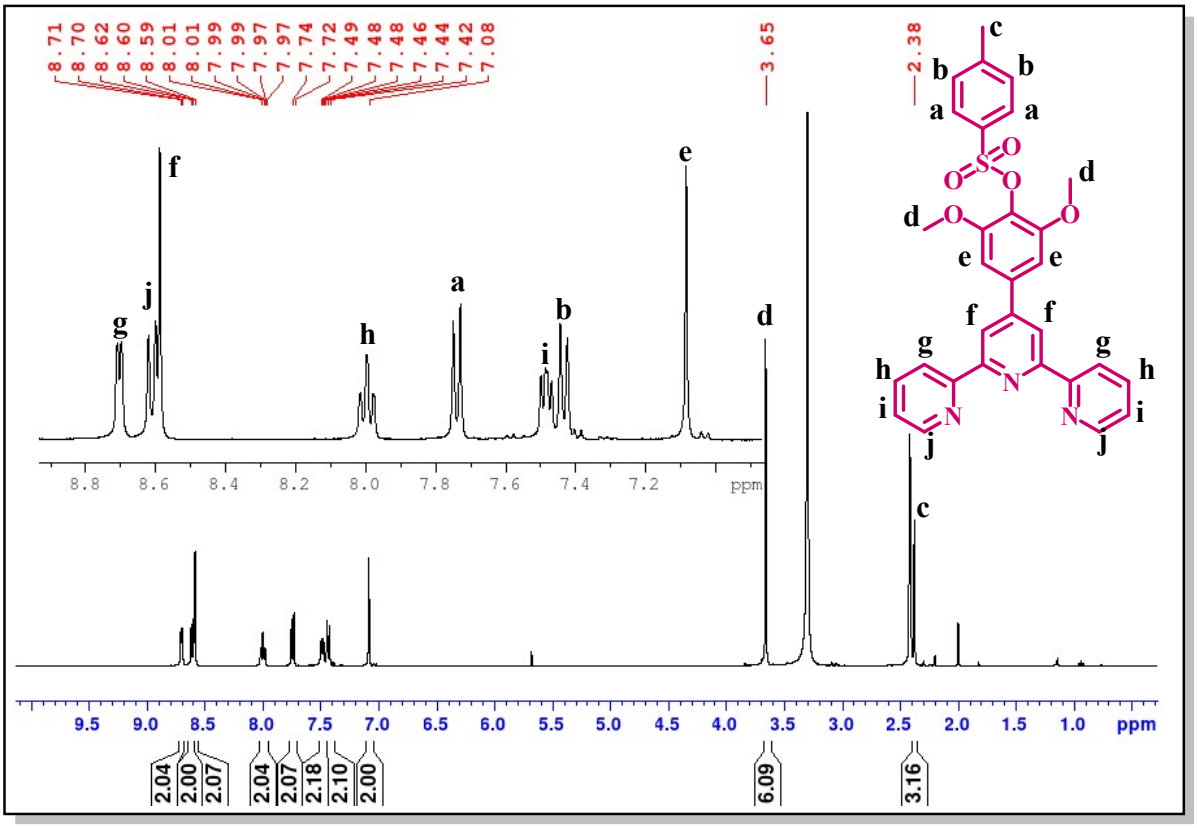

Figure S9. [1]H NMR Spectrum of compound **L3**

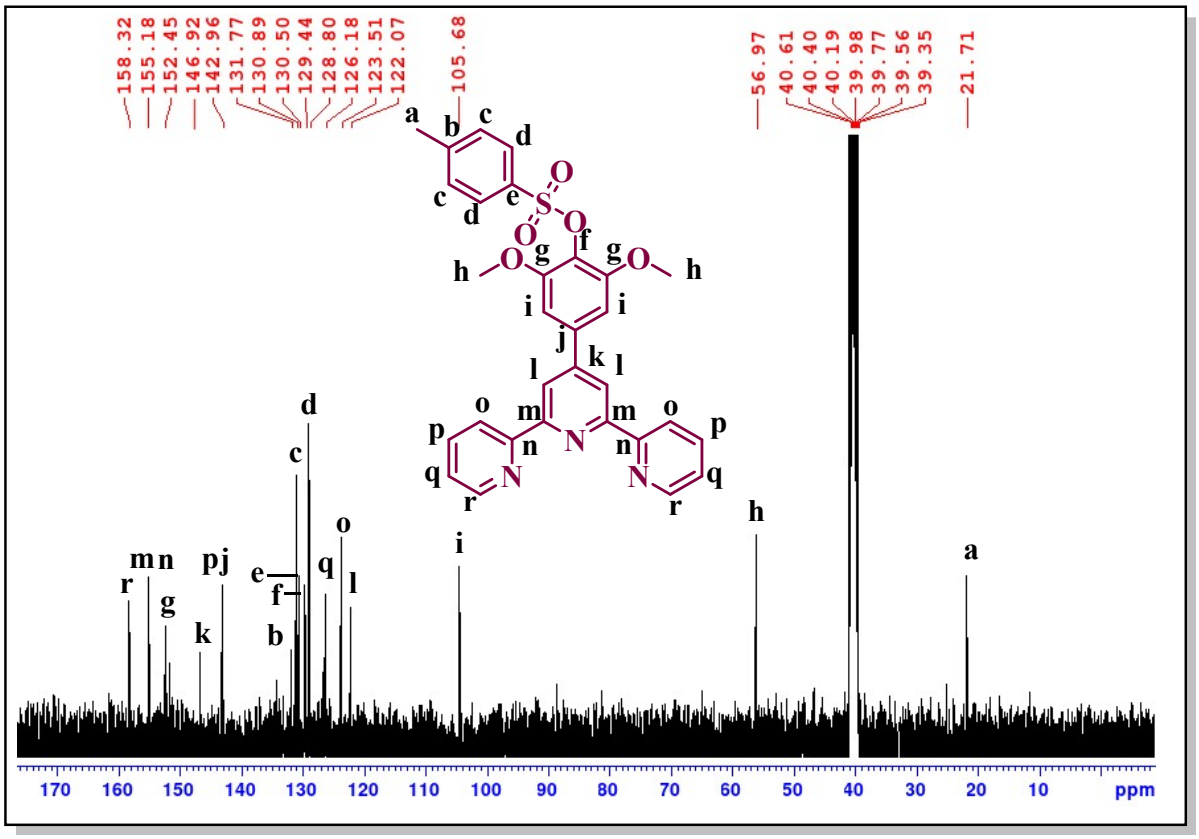

Figure S10. ^{13}C NMR Spectrum of compound **L3**

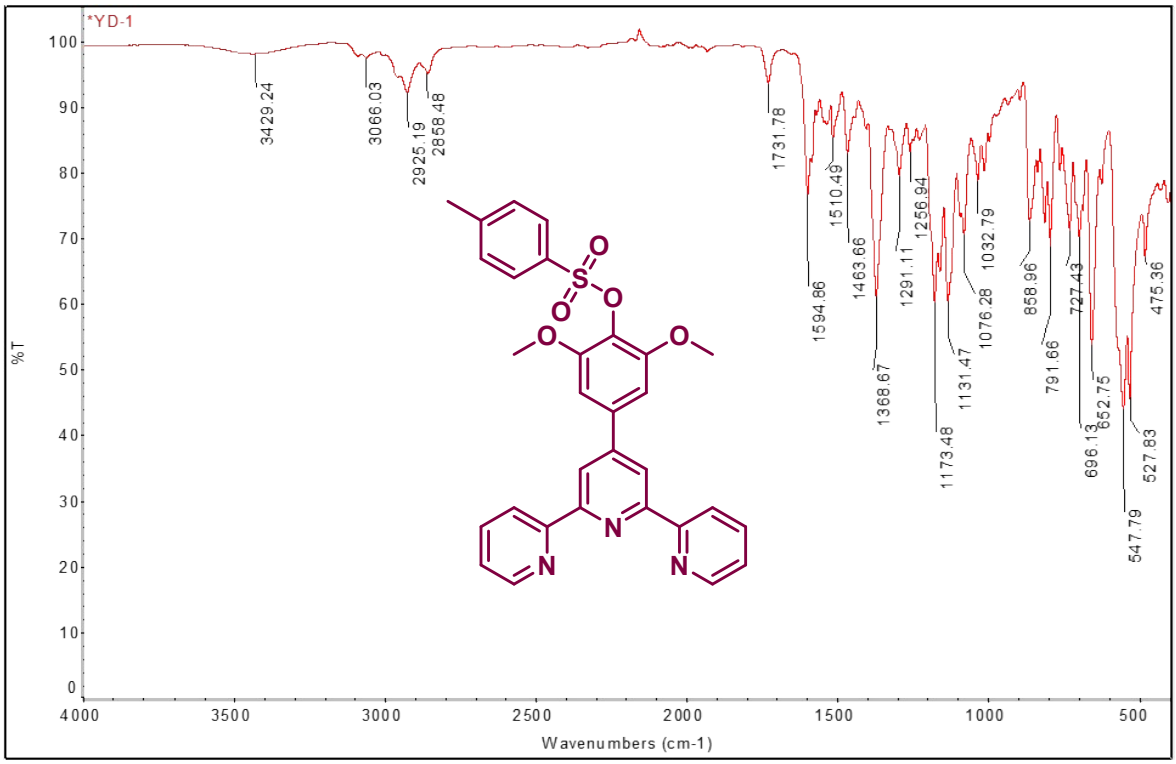

Figure S11. IR Spectrum of compound **L3**

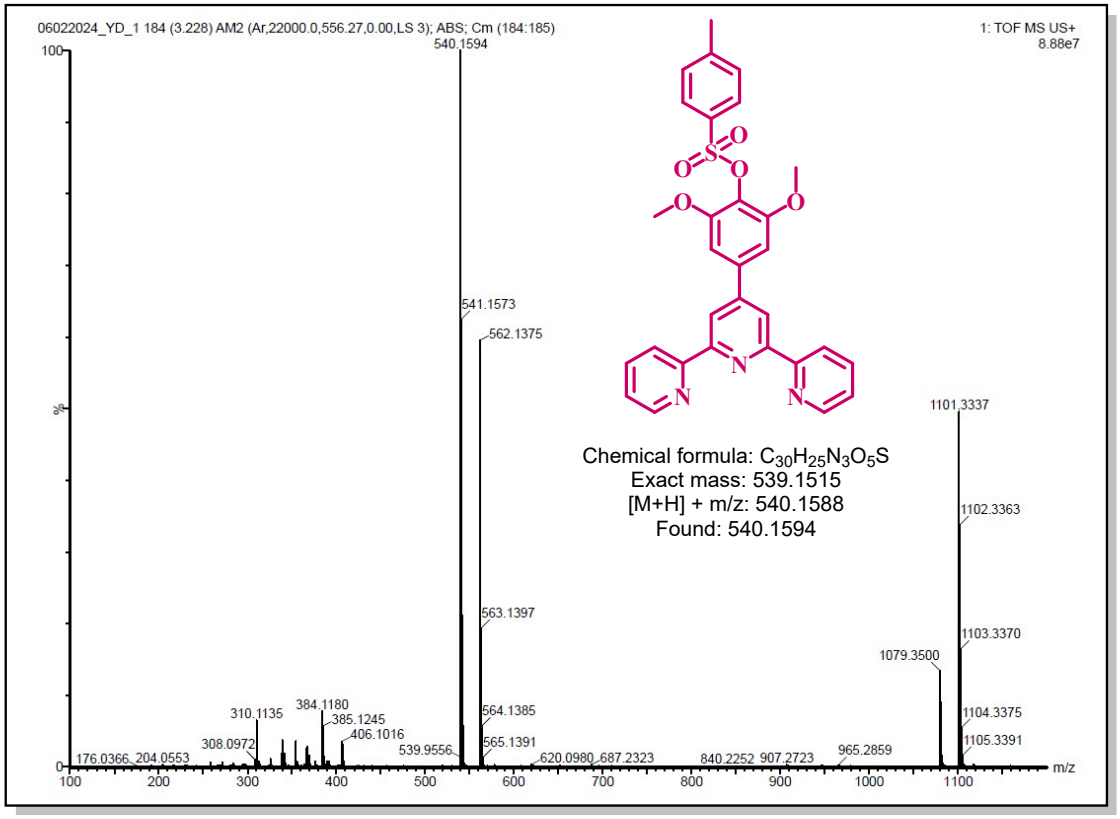

Figure S12. ESI-Mass Spectrum of compound **L3**

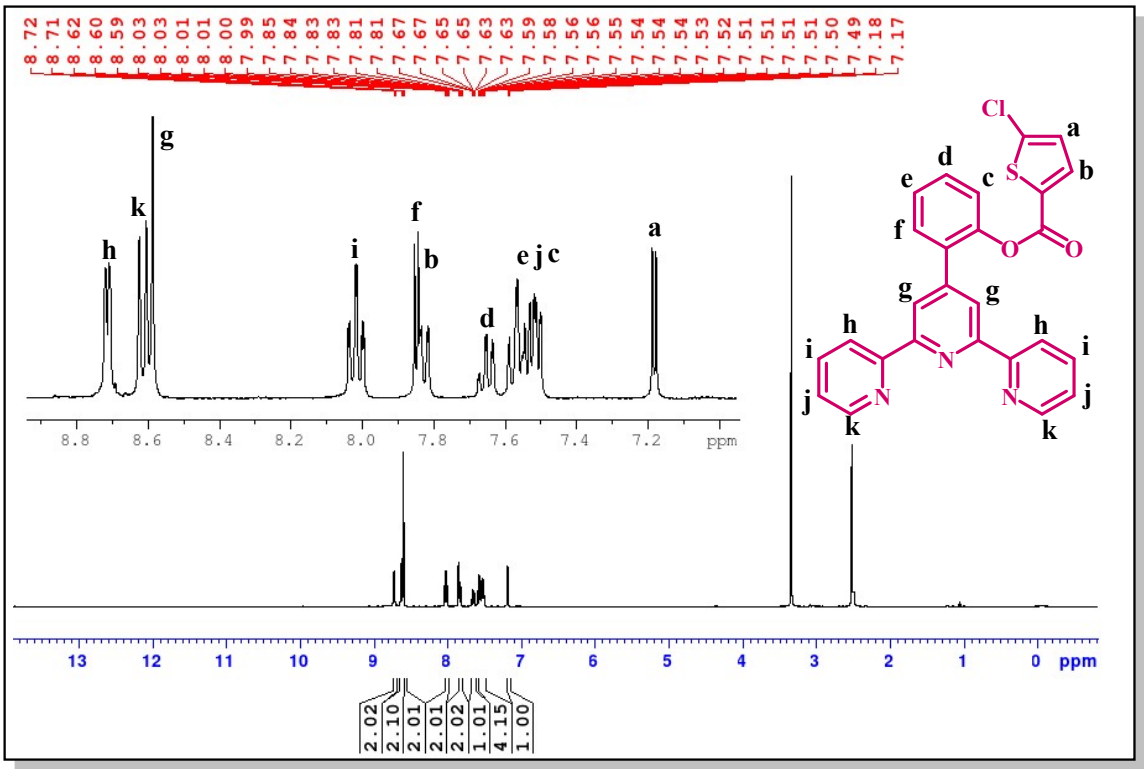

Figure S13. ^{1}H NMR Spectrum of compound **L4**

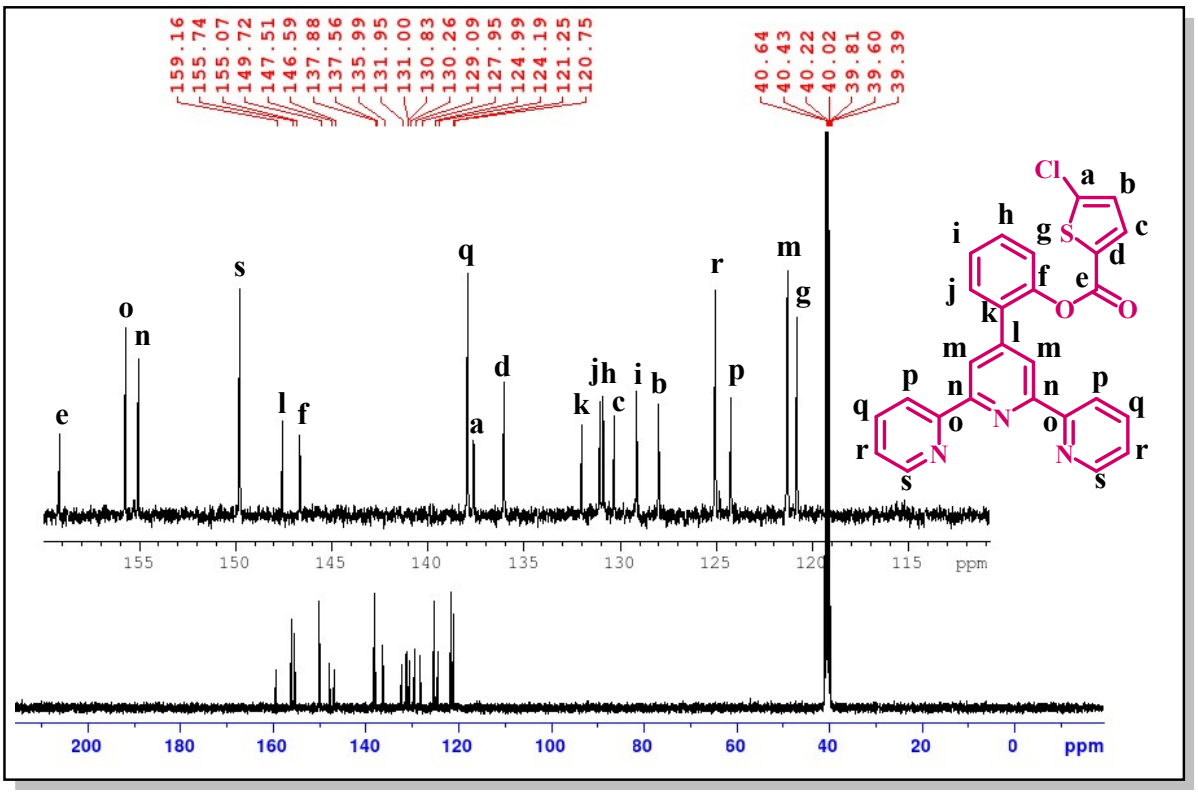

Figure S14. ^{13}C NMR Spectrum of compound **L4**

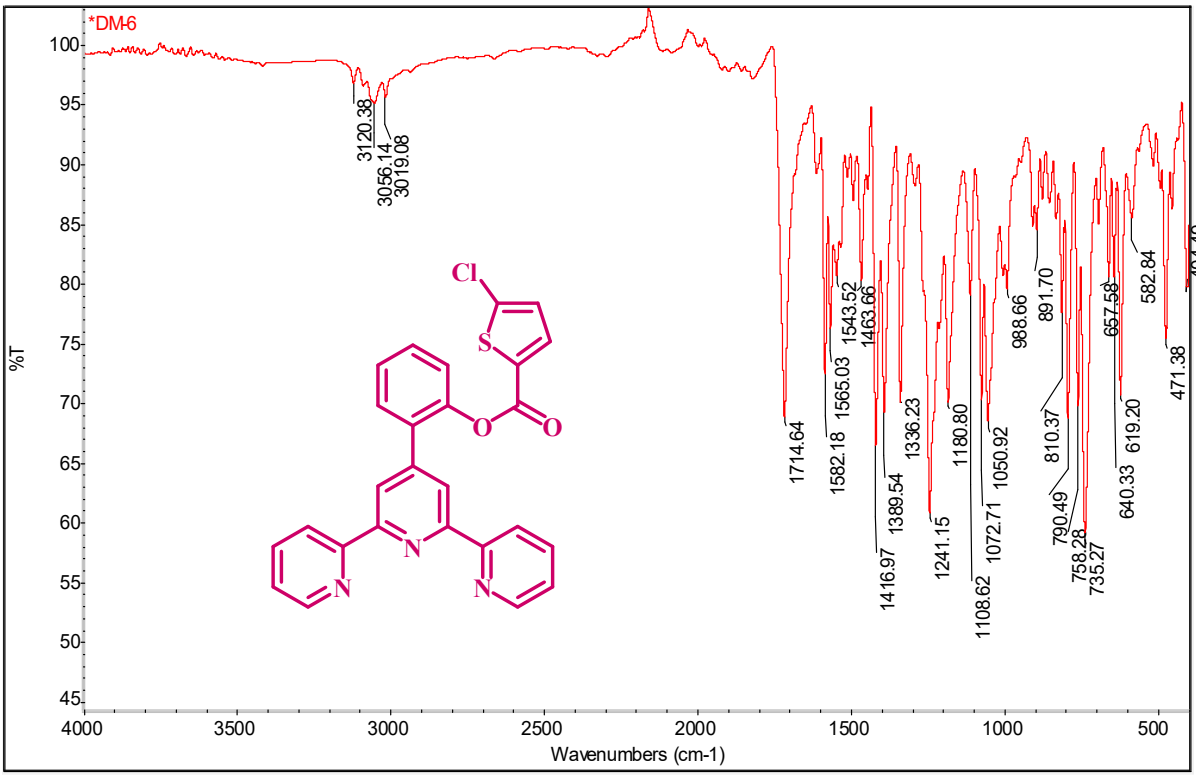

Figure S15. IR Spectrum of compound **L4**

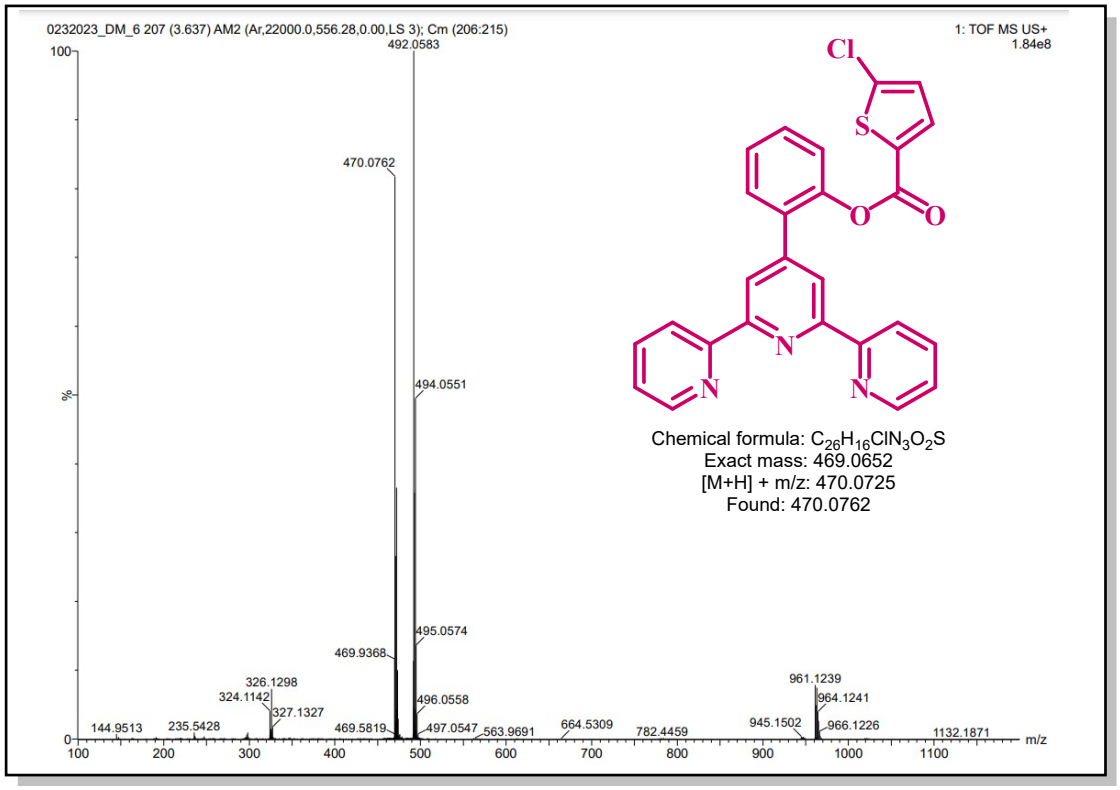

Figure S16. ESI-Mass Spectrum of compound **L4**

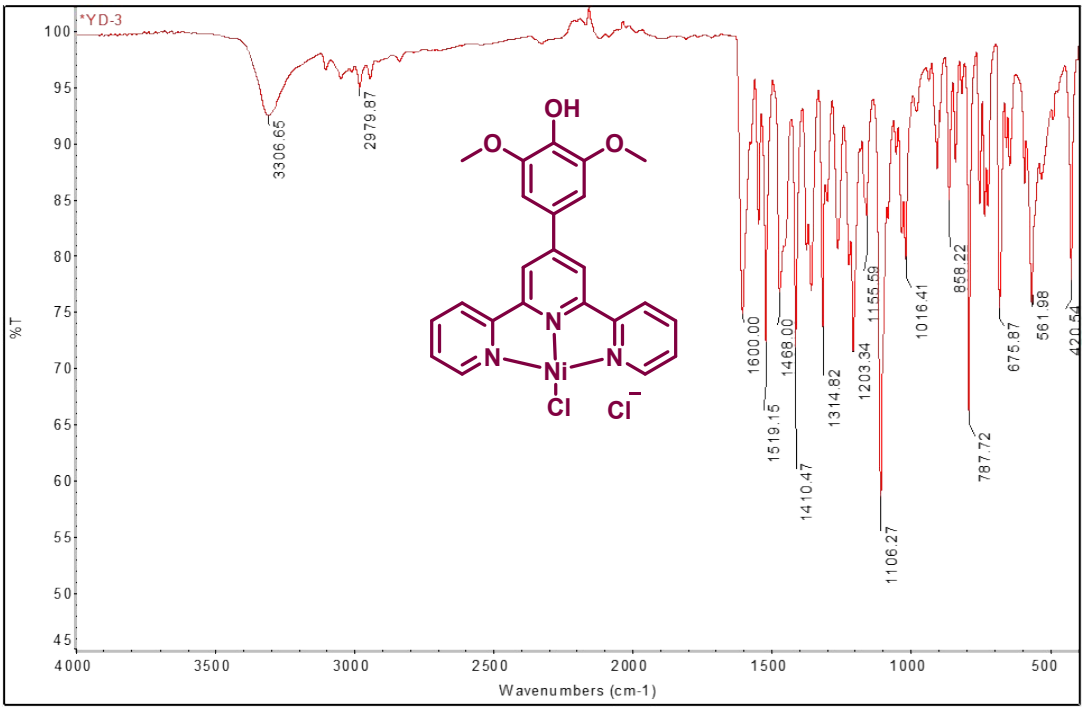

Figure S17. IR Spectrum of compound **NiL1**

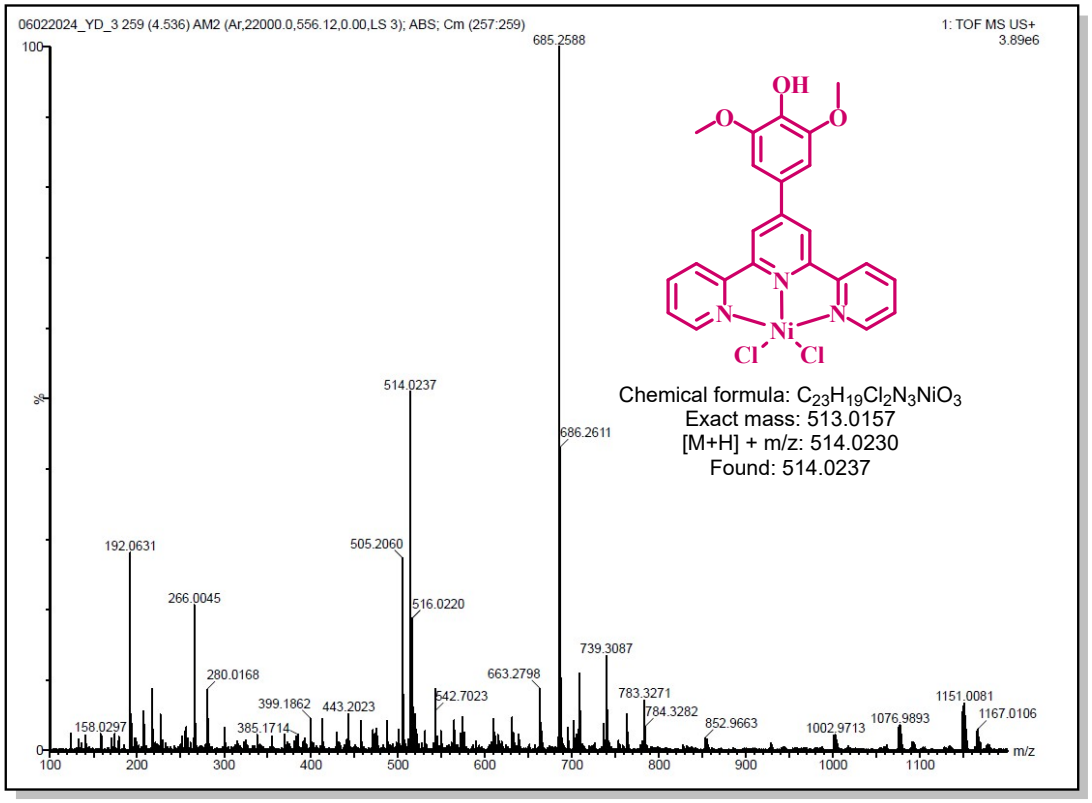

Figure S18. ESI-Mass Spectrum of compound **NiL1**

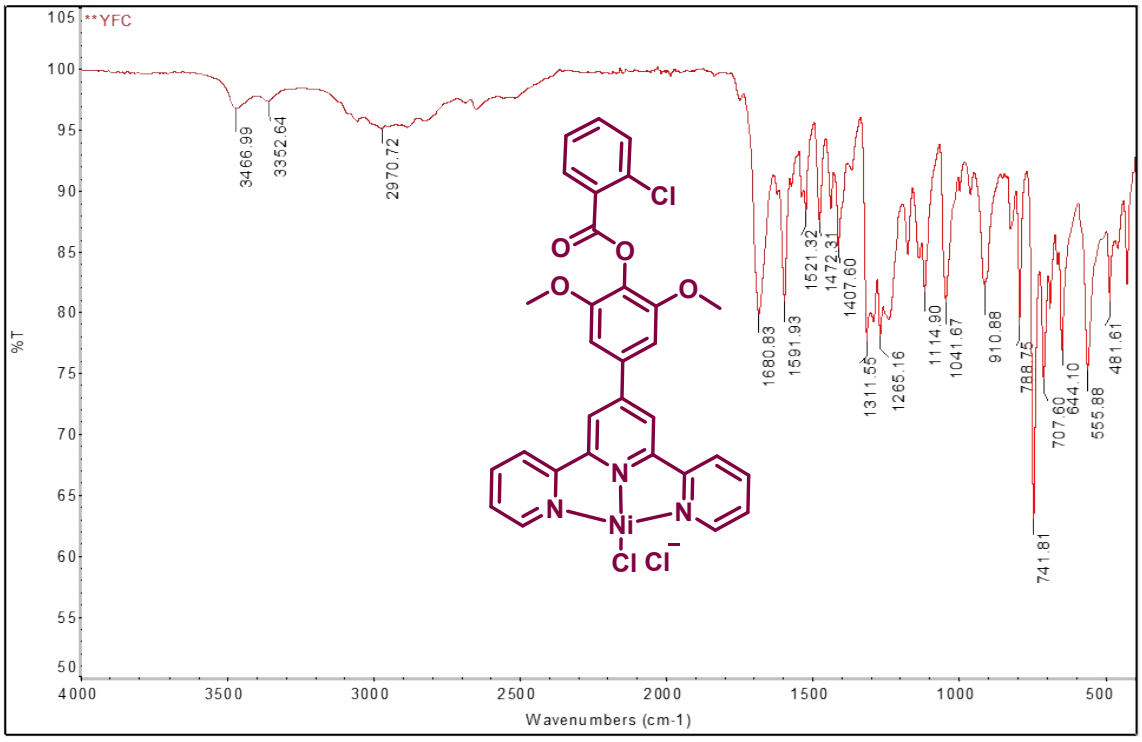

Figure S19. IR Spectrum of compound **NiL2**

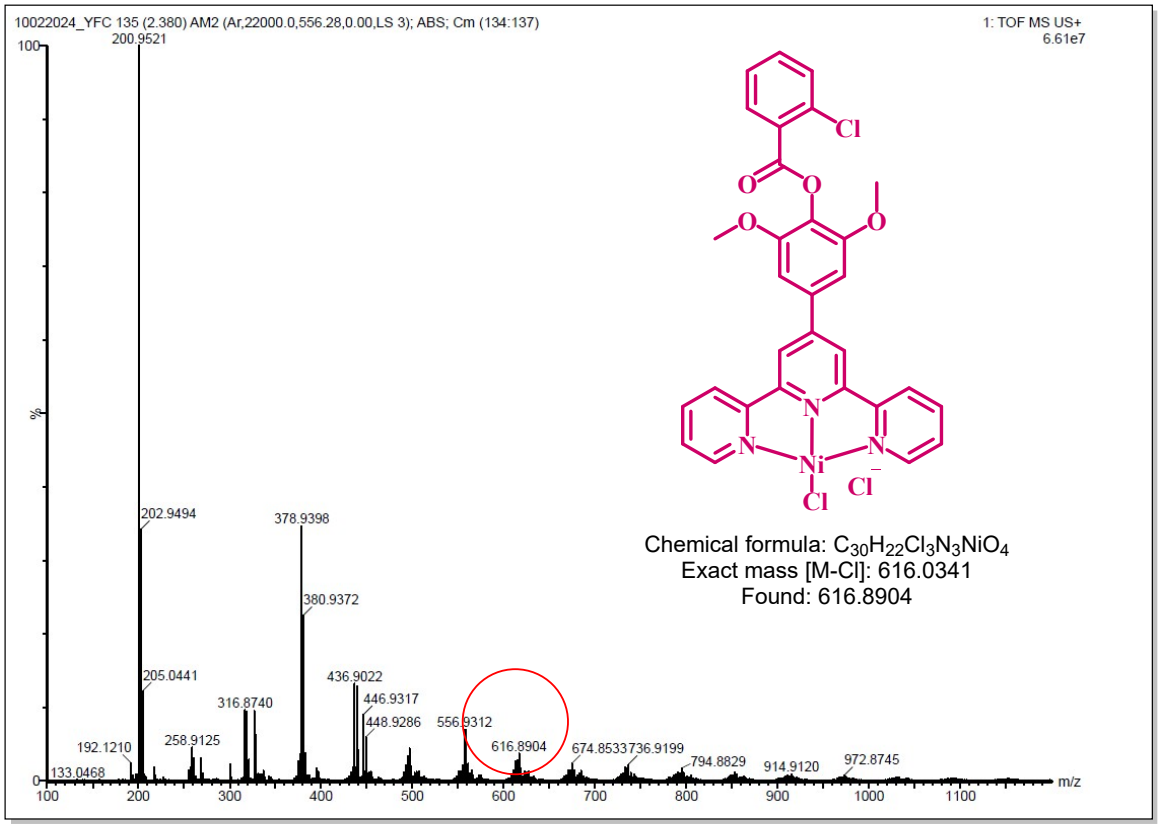

Figure S20. ESI-Mass Spectrum of compound **NiL2**

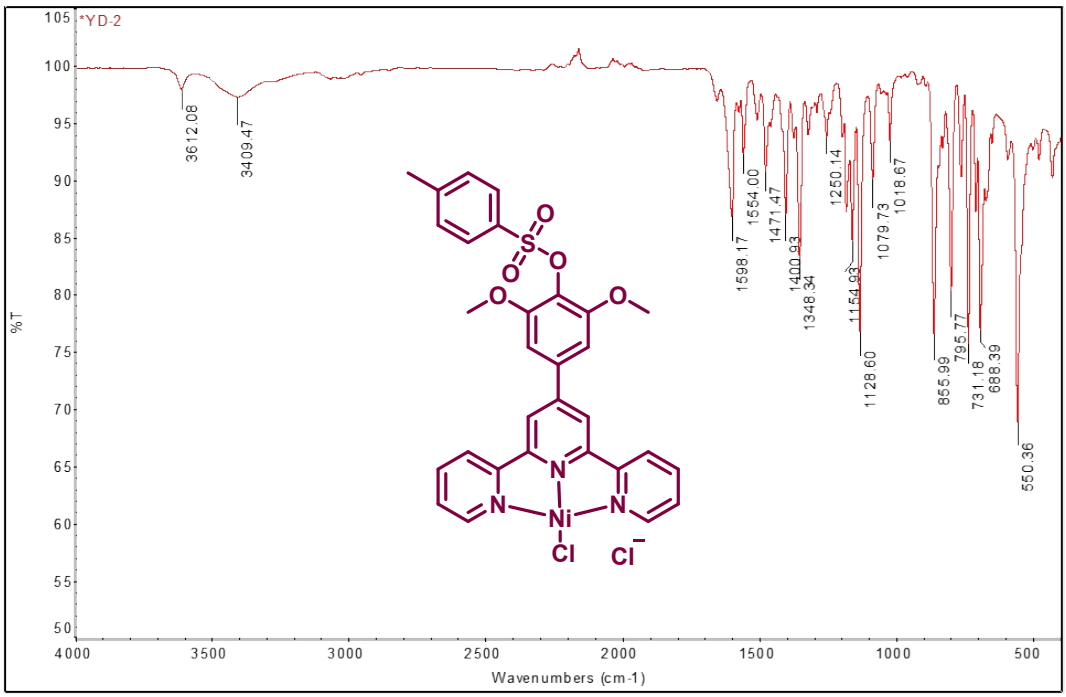

Figure S21. IR Spectrum of compound **NiL3**

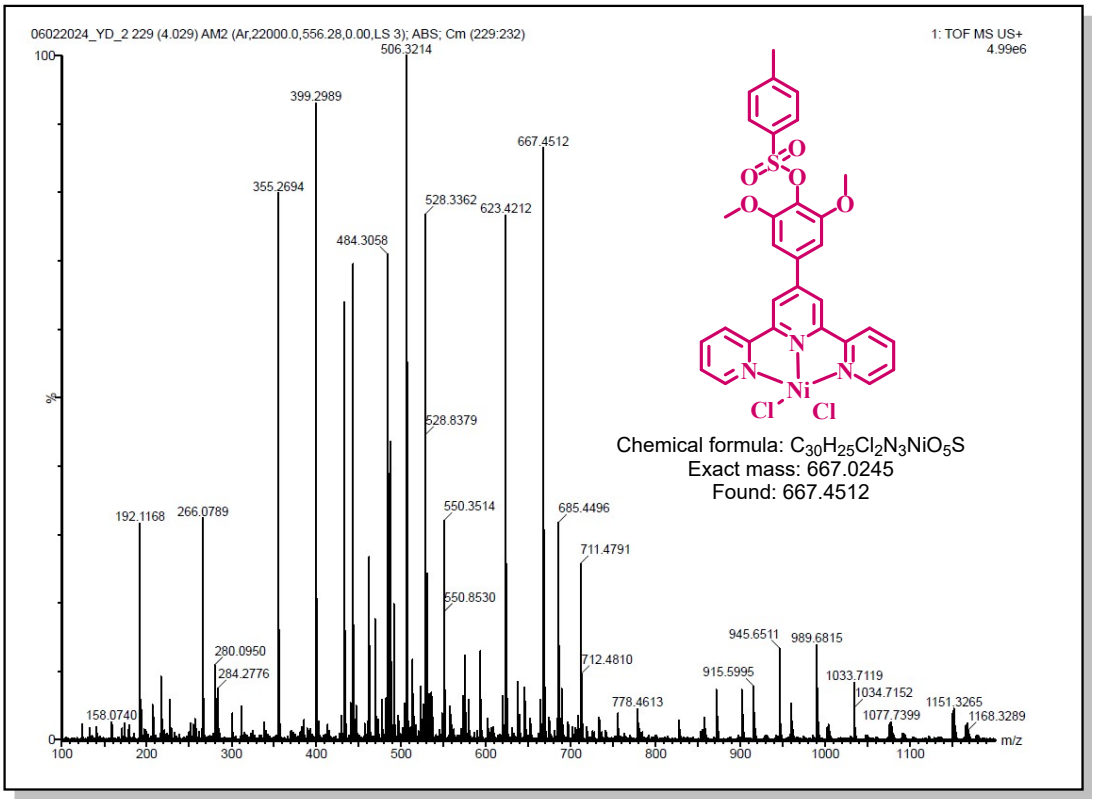

Figure S22. ESI-Mass Spectrum of compound **NiL3**

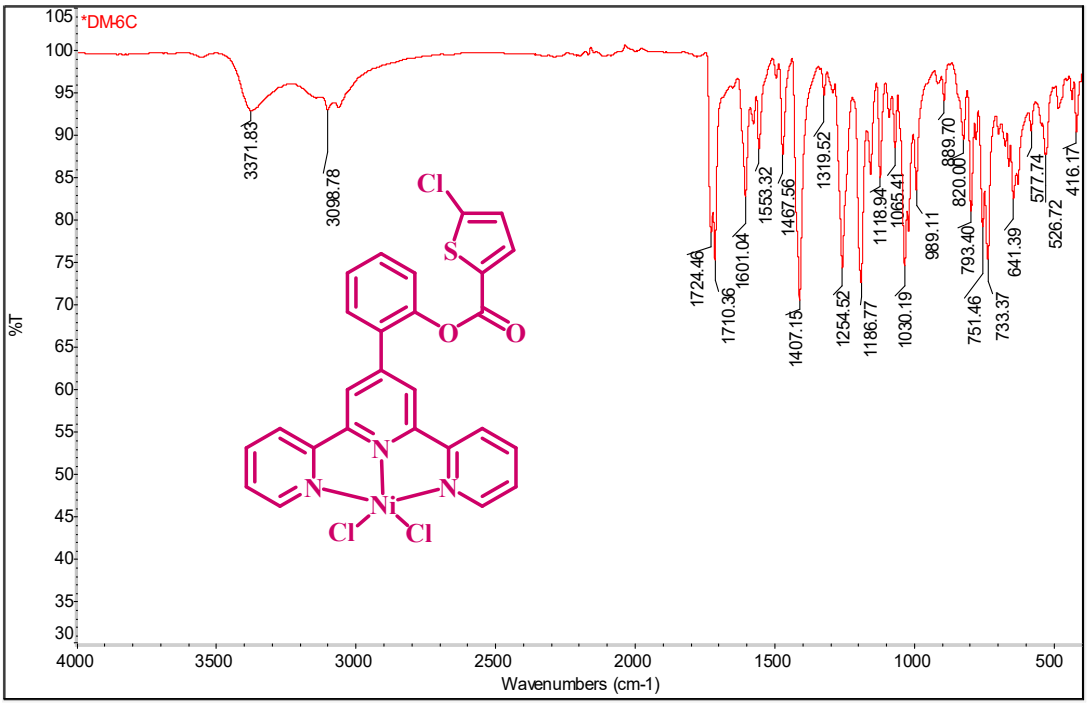

Figure S23. IR Spectrum of compound **NiL4**

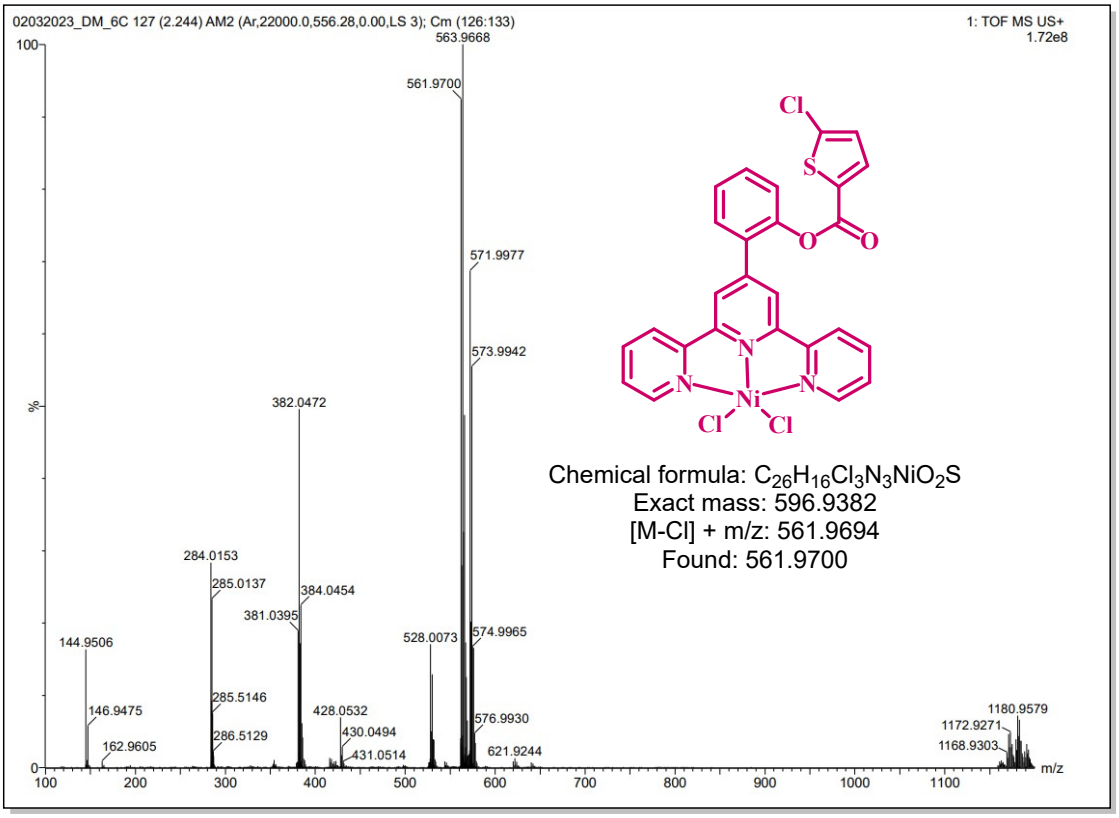

Figure S24. ESI-Mass Spectrum of compound **NiL4**

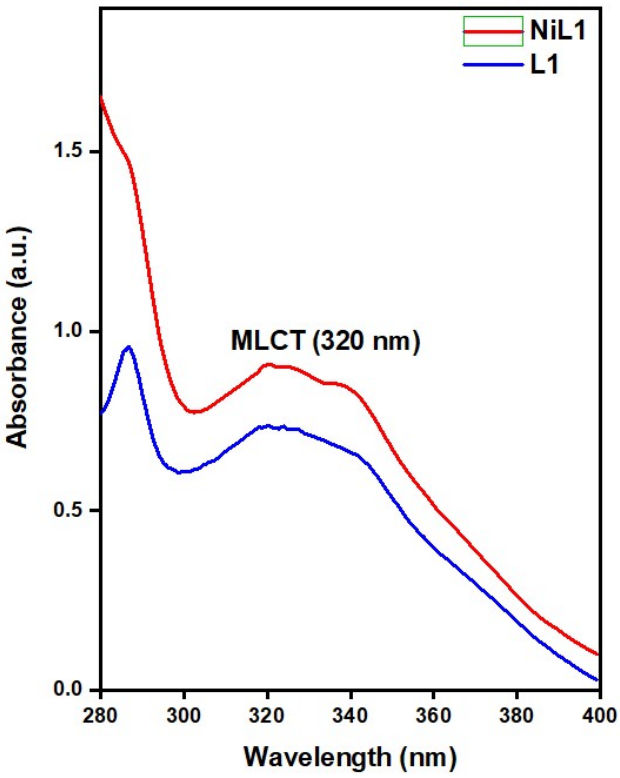

Figure S25. UV-Visible Spectra of compound **L1** and **NiL1**

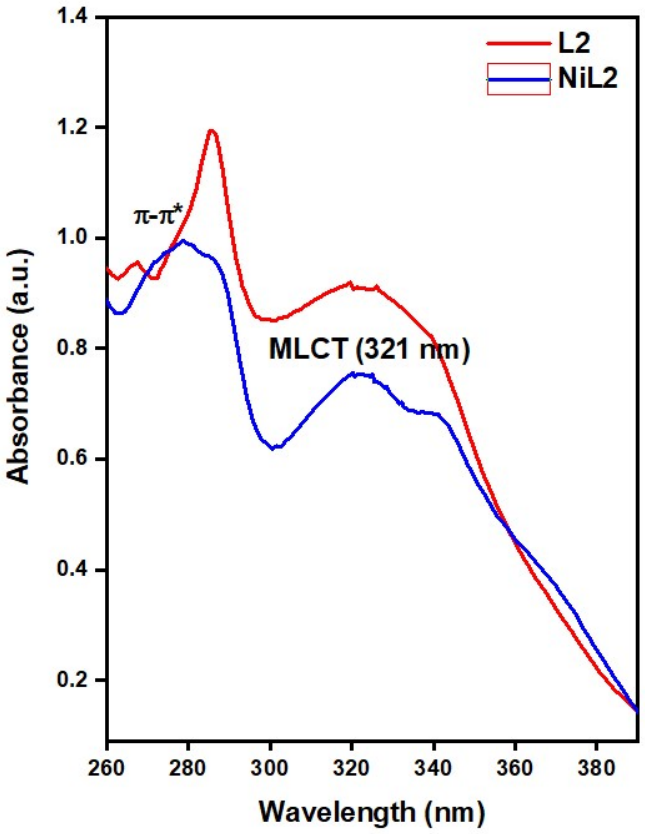

Figure S26. UV-Visible Spectra of compound **L2** and **NiL2**

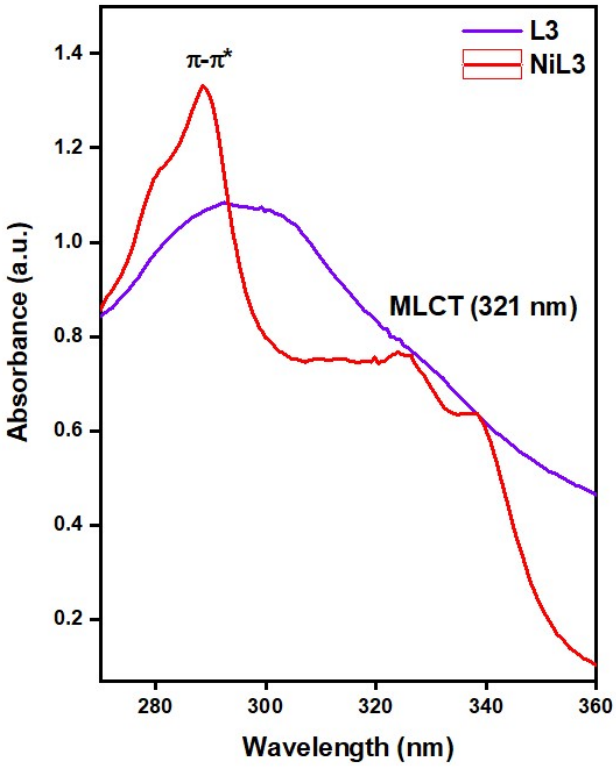

Figure S27. UV-Visible Spectra of compound **L3** and **NiL3**

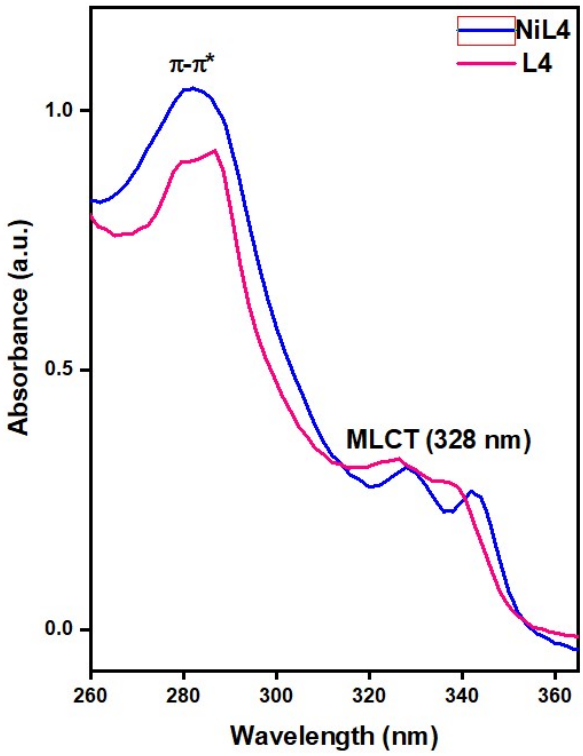

Figure S28. UV-Visible Spectra of compound **L4** and **NiL4**

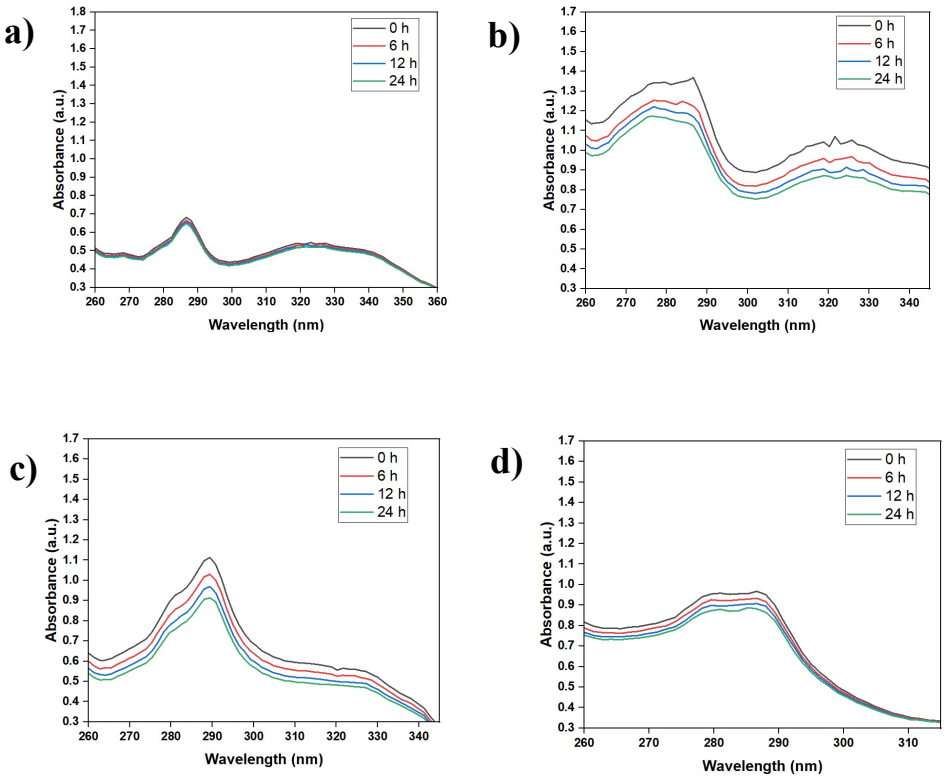

Figure S29. Stability studies of **L1-L4** (In order a-d) using UV–Visible absorption spectral data (1×10^{-5} M) in 0.1 mM glutathione (GSH)

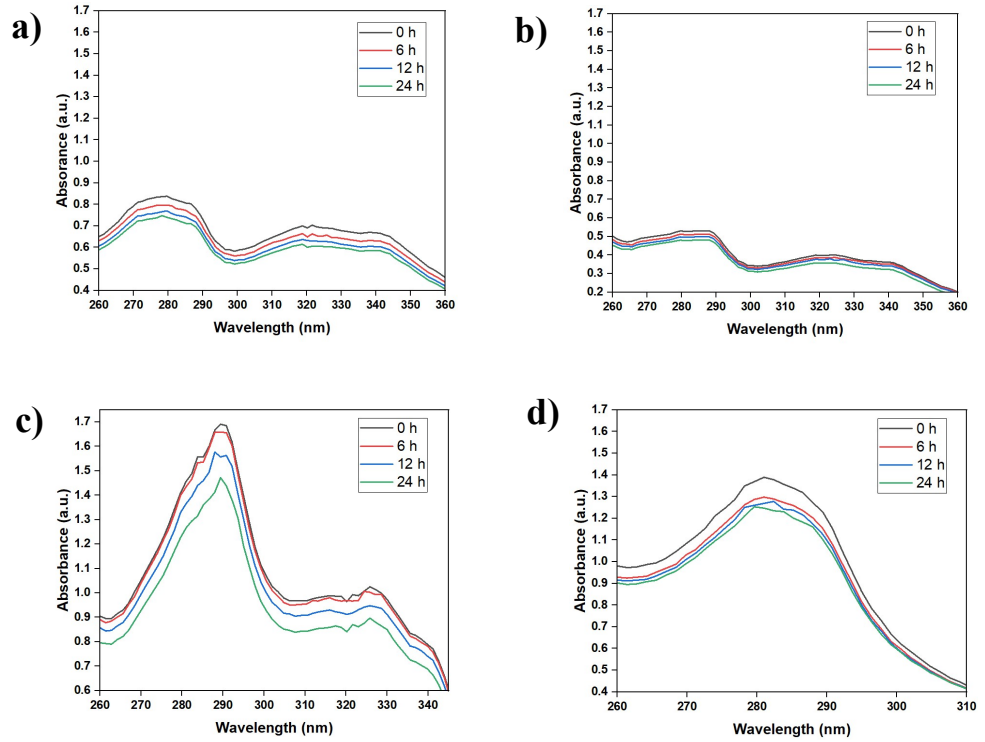

Figure S30. Stability studies of **NiL1-NiL4** (In order a-d) using UV–Visible absorption spectral data (1×10^{-5} M) in 0.1 mM glutathione (GSH)

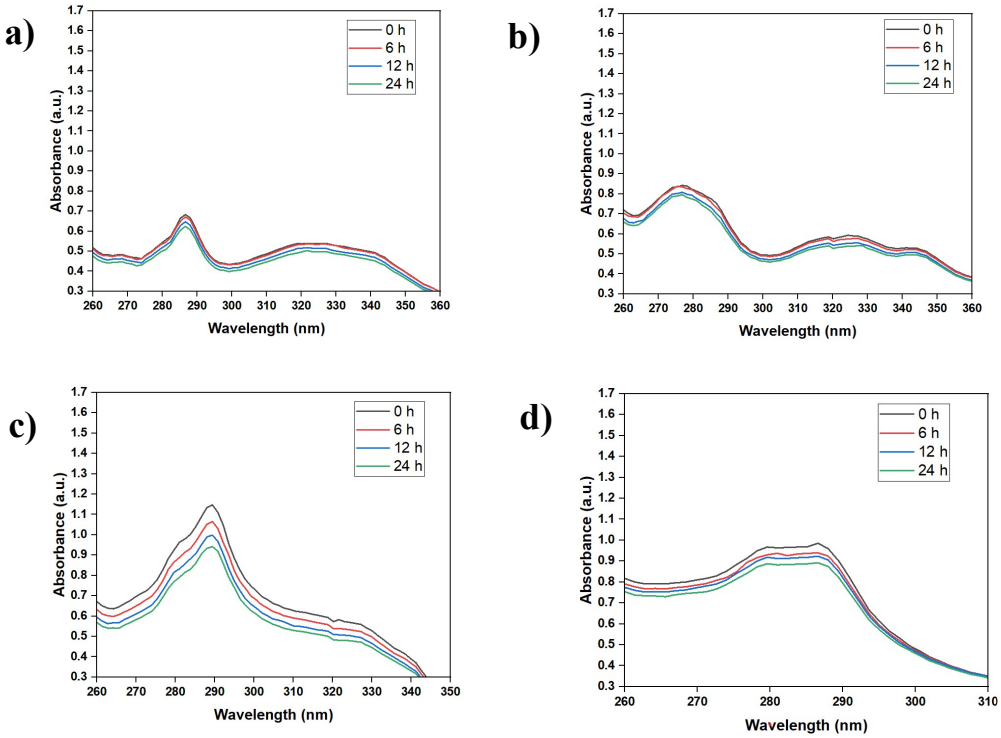

Figure S31. Stability studies of **L1-L4** (In order a-d) using UV–Visible absorption spectral data (1×10^{-5} M) under MTT conditions (*i.e.* 5% DMSO in phosphate buffer)

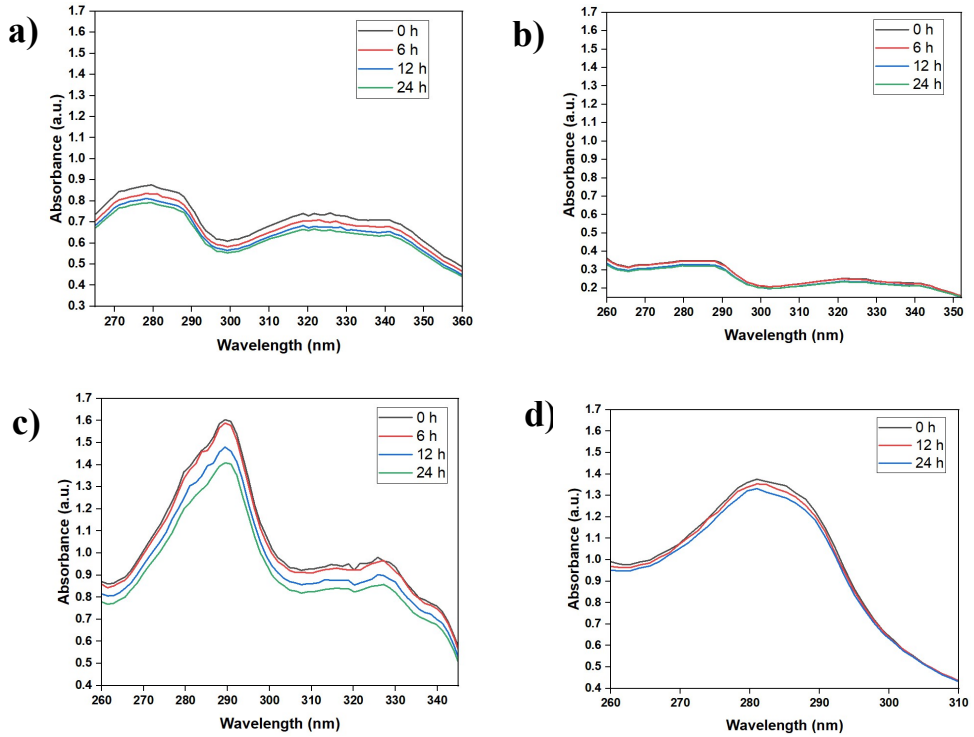

Figure S32. Stability studies of **NiL1-NiL4** (In order a-d) using UV–Visible absorption spectral data (1×10^{-5} M) under MTT conditions (*i.e.* 5% DMSO in phosphate buffer)

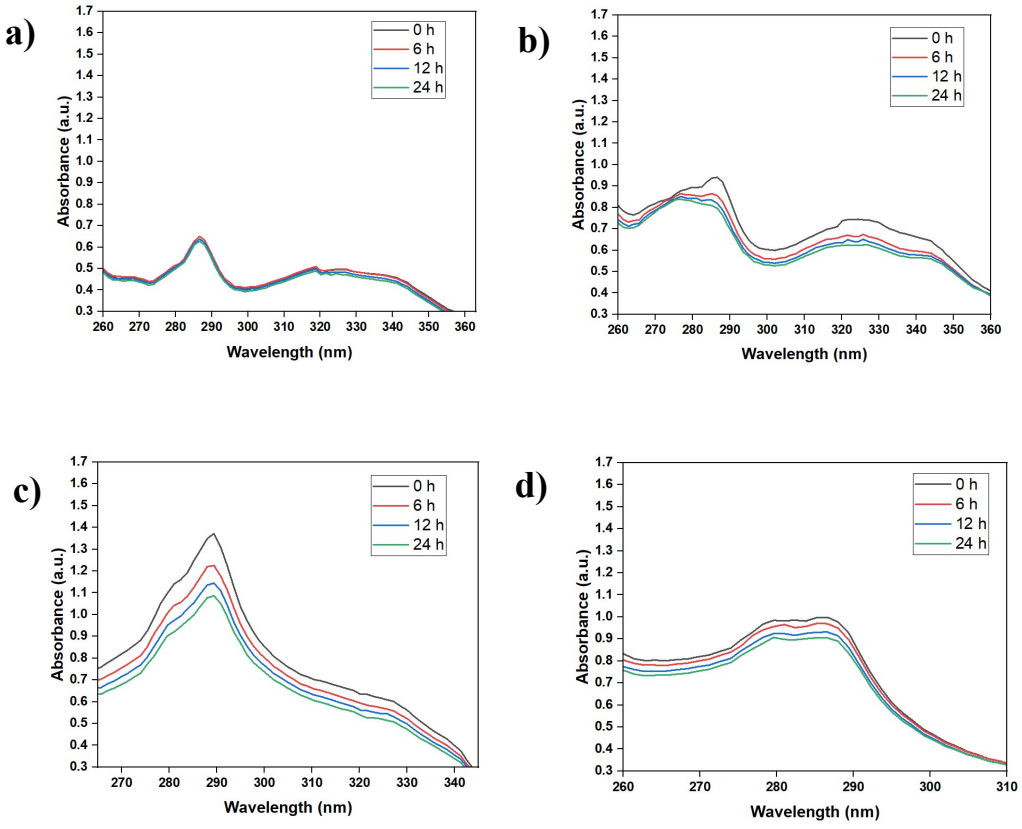

Figure S33. Stability studies of **L1-L4** (In order a-d) using UV–Visible absorption spectral data (1×10^{-5} M) in water

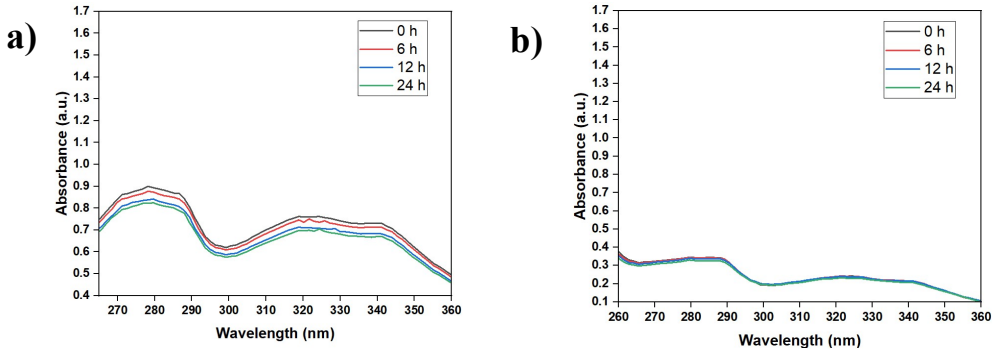

Figure S34. Stability studies of **NiL1-NiL4** (In order a-d) using UV–Visible absorption spectral data (1×10^{-5} M) in water

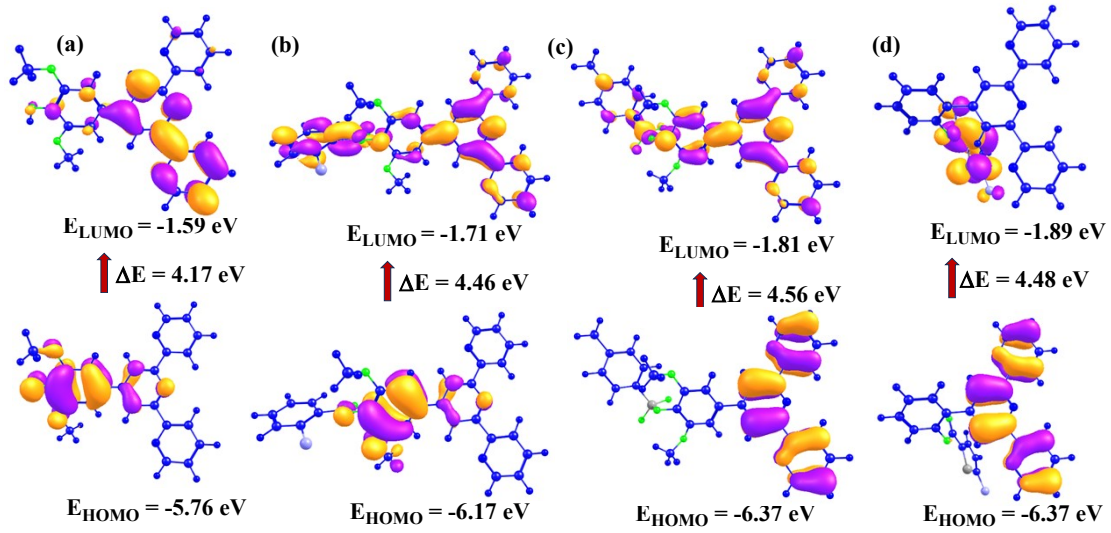

Figure S35. Frontier molecular orbitals of the complexes **L1** (a), **L2** (b), **L3** (c) and **L4** (d)

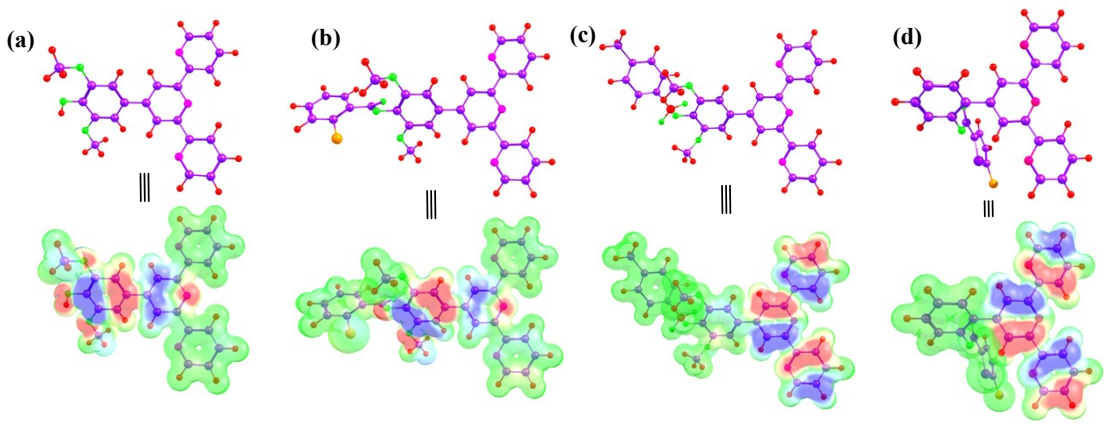

Figure S36 The ESP mapped on the surface of the ligand **L1** (a), **L2** (b), **L3** (c) and **L4** (d) by the DFT-B3LYP method

Table S1 Binding energy values of the synthesized ligands and complexes with BSA, 1m17-3 and DNA (AT Rich, GC Rich and Mixed)

. No	Compound	BSA	1m17-3	DNA		
				AT Rich	GC Rich	Mixed
1	**L1**	-10.1	-9.3	-7.6	-7.1	-8.7
2	**L2**	-10.3	-9.7	-8.0	-7.8	-8.6
3	**L3**	-10.6	-10.5	-8.0	-8.1	-8.7
4	**L4**	-9.0	-10.6	-7.3	-7.3	-6.5
5	**NiL1**	-8.8	-9.7	-8.1	-7.6	-7.8
6	**NiL2**	-10.3	-10.5	-8.2	-8.3	-8.7
7	**NiL3**	-10.4	-9.6	-8.6	-8.9	-9.2
8	**NiL4**	-9.0	-9.8	-7.3	-7.4	-8.2

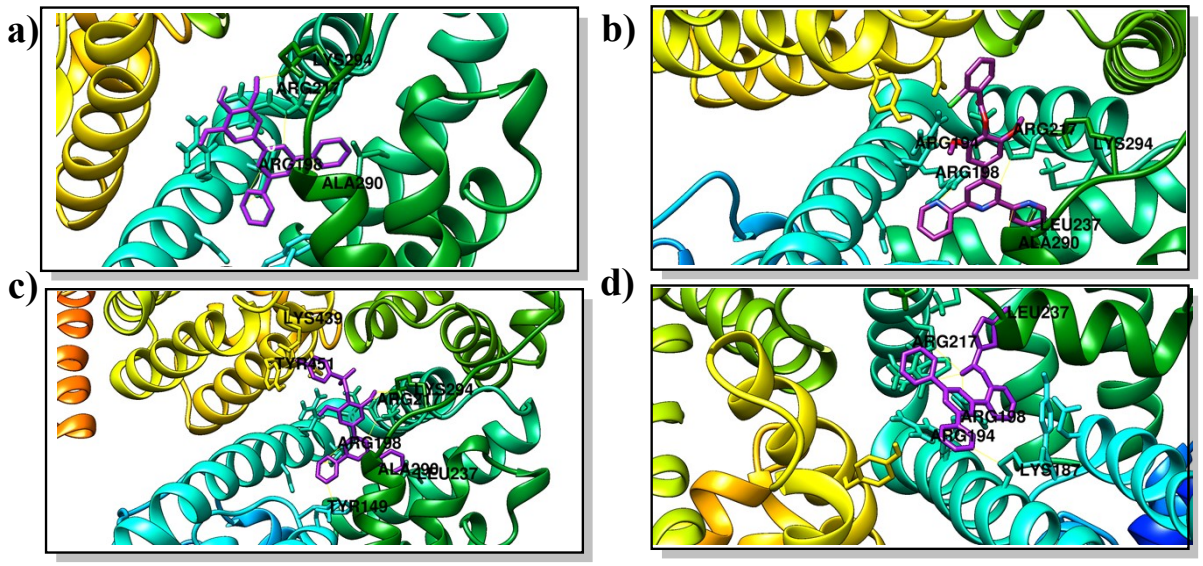

Figure S37 Molecular docking interactions of ligands with BSA

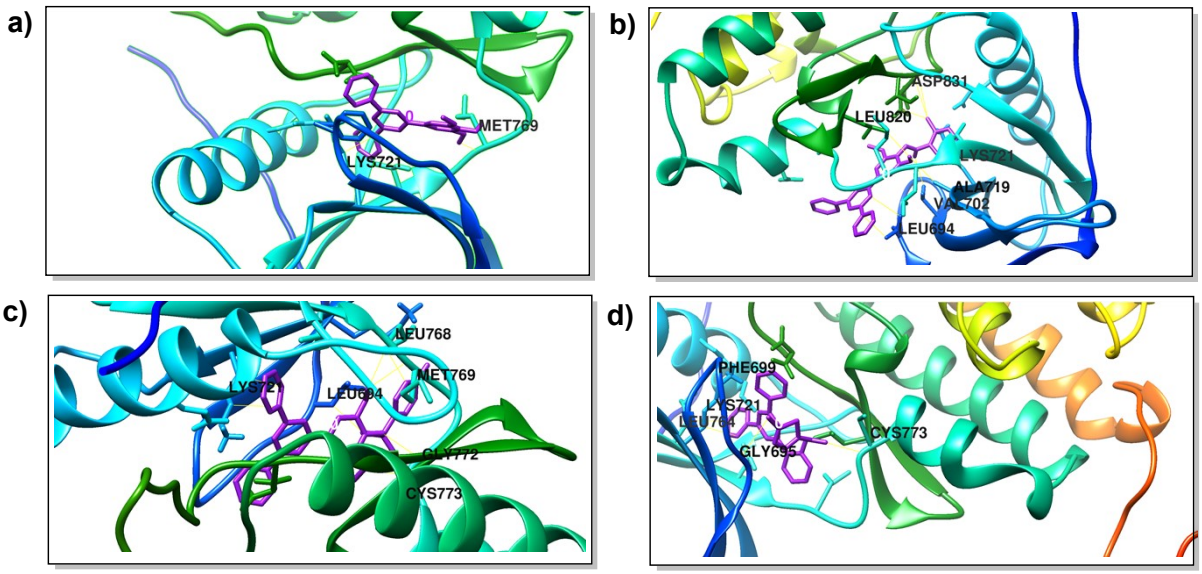

Figure S38 Molecular docking interactions of ligands with Im-17-3

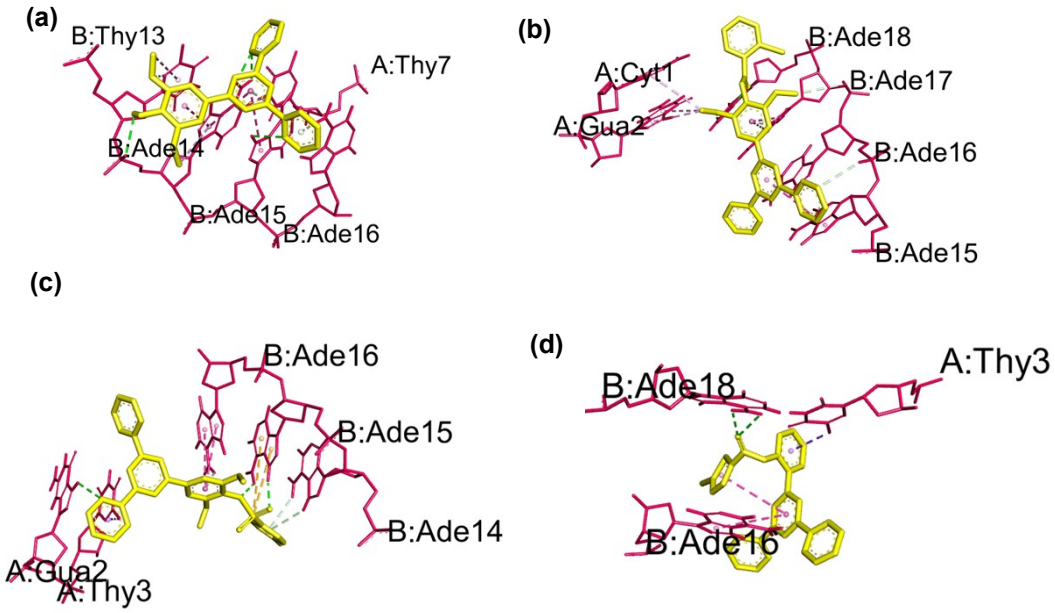

Figure S39. Molecular docking interactions of ligands with DNA (AT Rich)

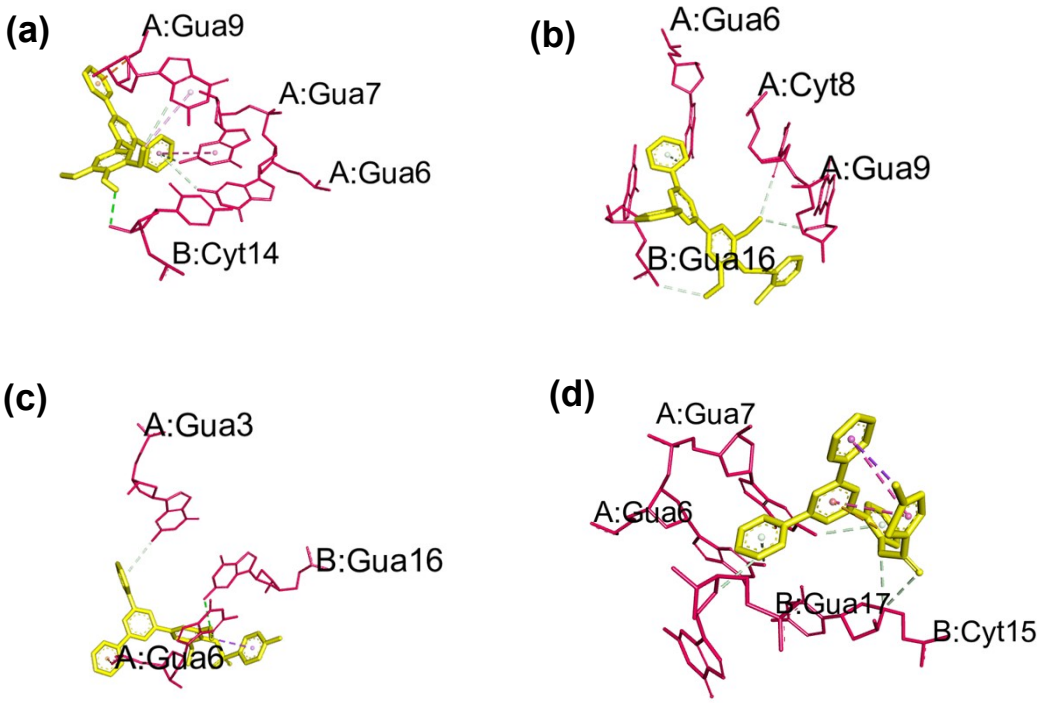

Figure S40. Molecular docking interactions of ligands with DNA (GC Rich)

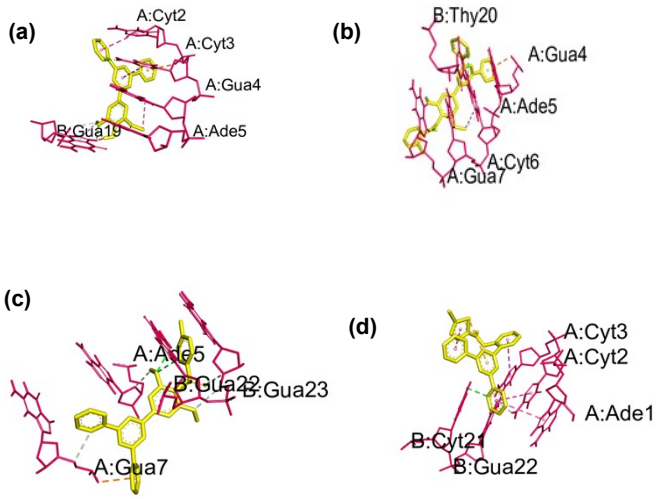

Figure S41. Molecular docking interactions of ligands with DNA (Mixed)

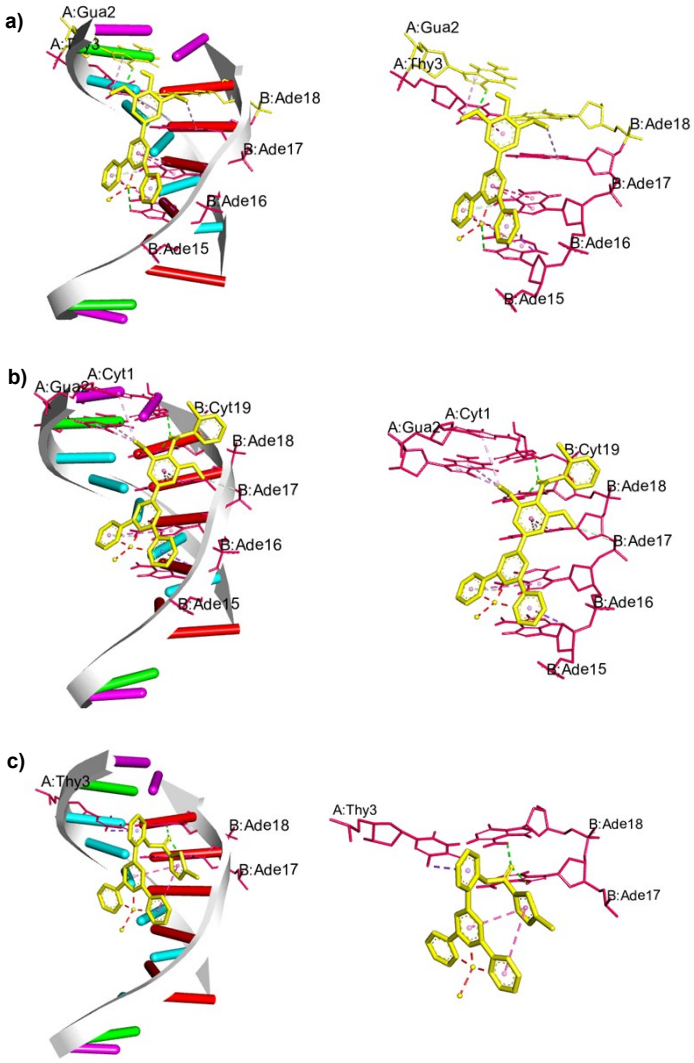

Figure S42. Molecular docking interactions of complexes **NiL1 (a), NiL2 (b), NiL4 (c)** with DNA (AT Rich)

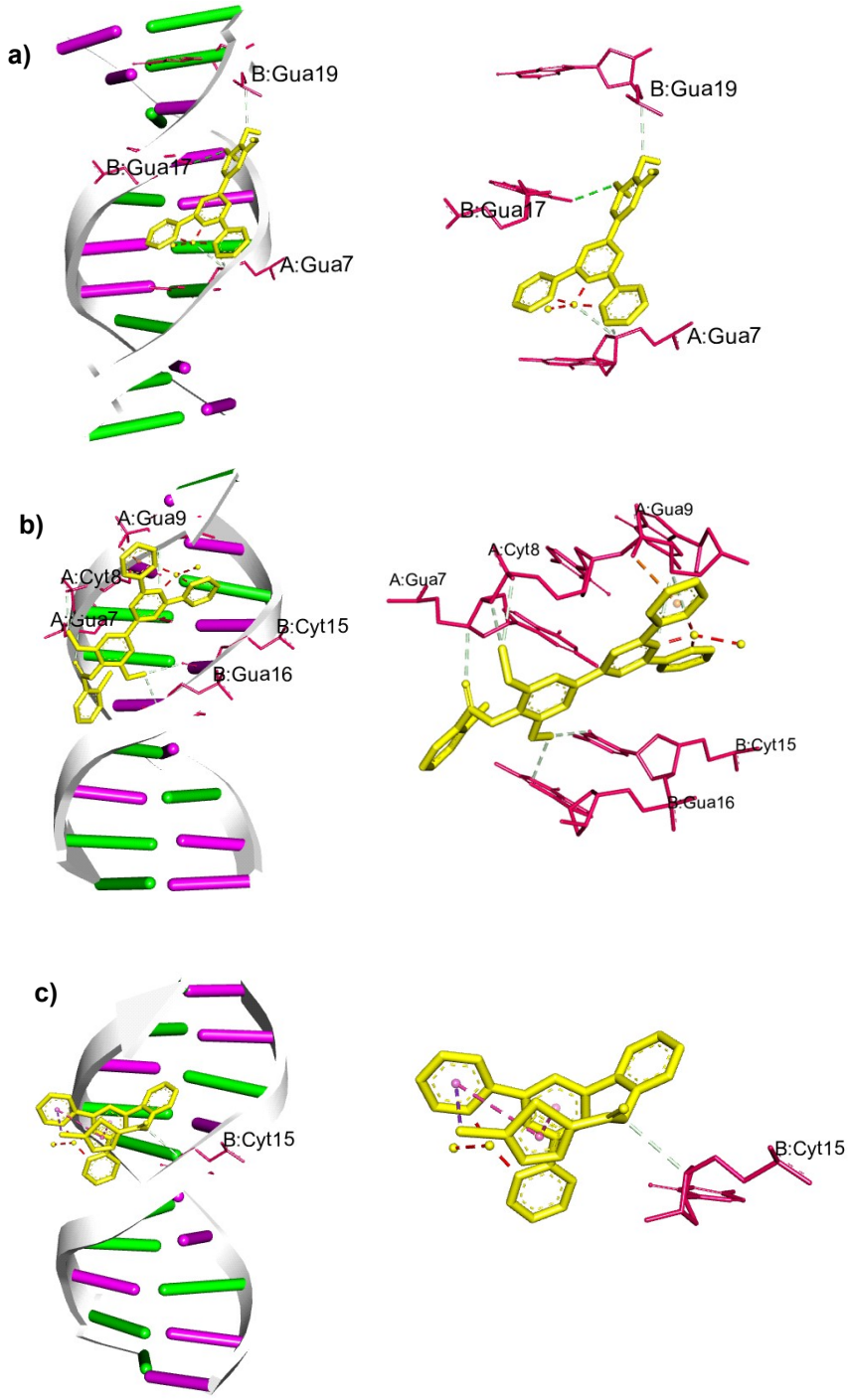

Figure S43. Molecular docking interactions of complexes **NiL1 (a), NiL2 (b), NiL4 (c)** with DNA (GC Rich)

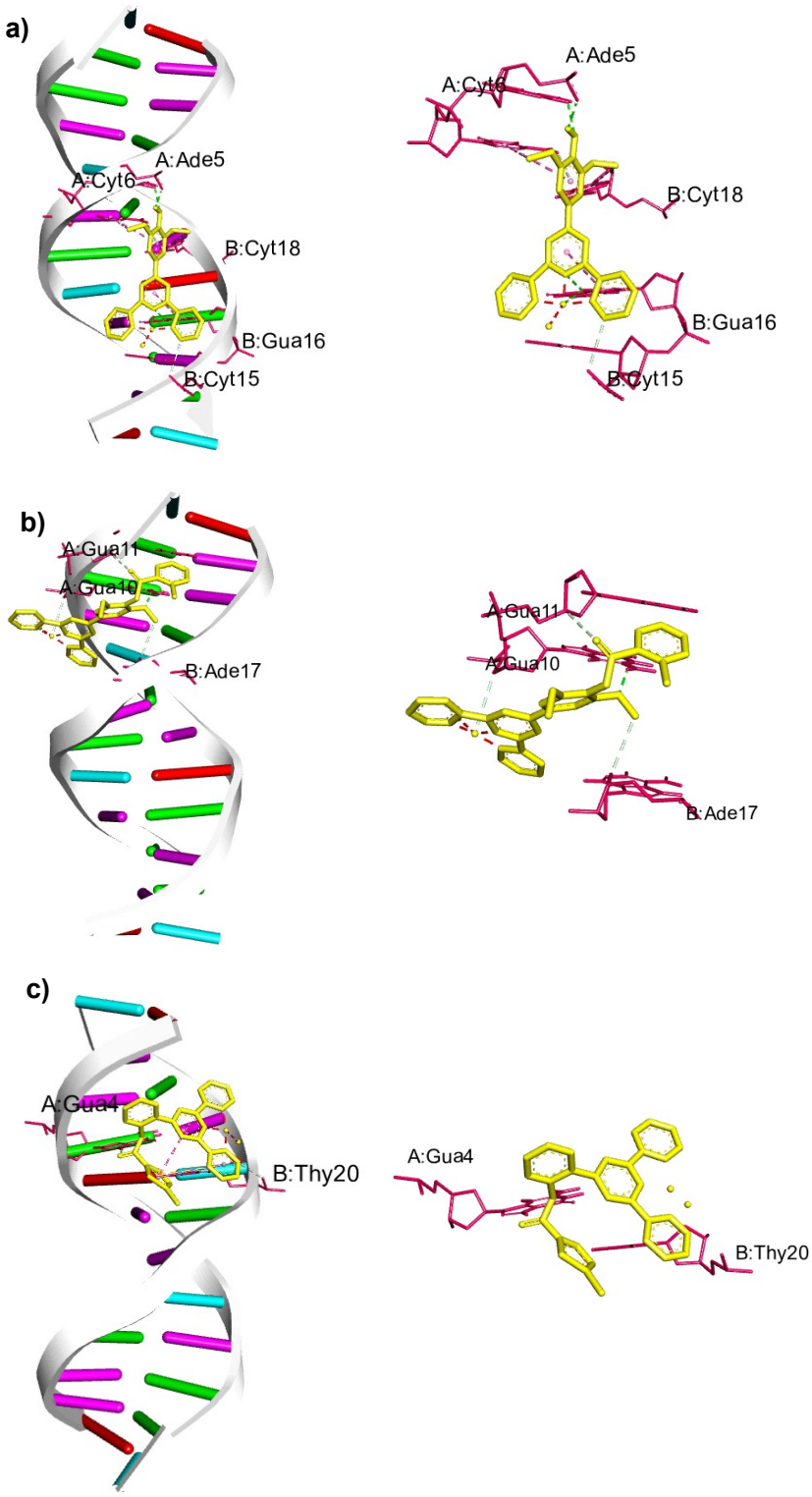

Figure S44. Molecular docking interactions of complexes **NiL1 (a), NiL2 (b), NiL4 (c)** with DNA (Mixed)

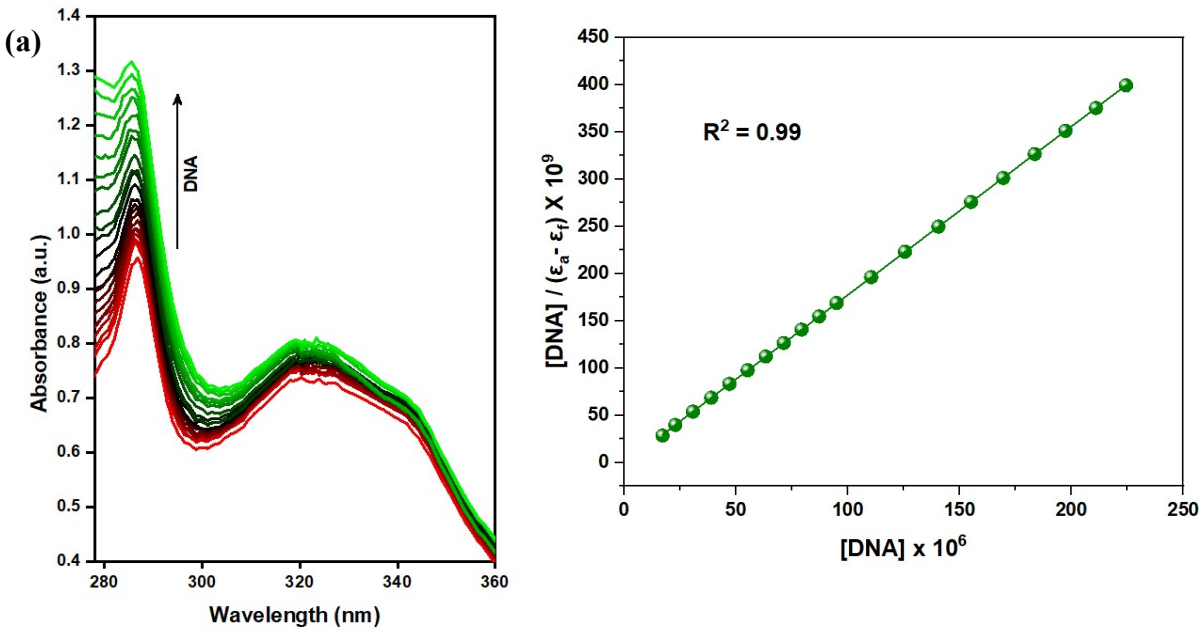

Figure S45. UV-Visible absorbance response of **L1** (1.0 x 10^{-5}) at pH 7.2 in 5 mM Tris-HCl-NaCl buffer solution in the presence of incremental addition of CT-DNA

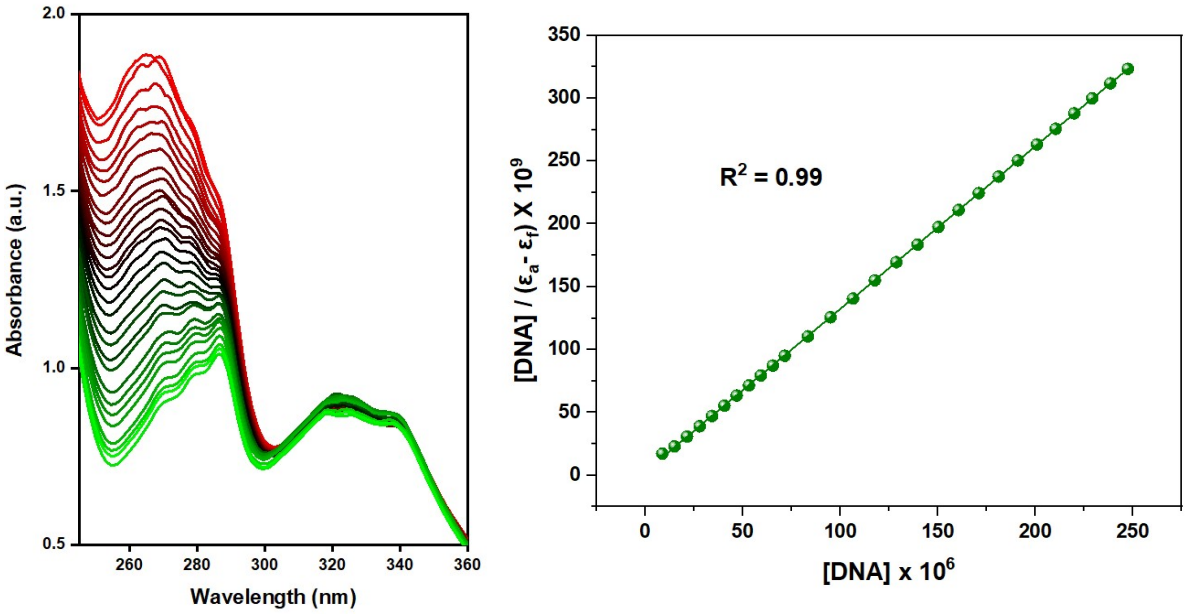

Figure S46. UV-Visible absorbance response of **NiL1** (1.0 x 10^{-5}) at pH 7.2 in 5 mM Tris-HCl-NaCl buffer solution in the presence of incremental addition of CT-DNA

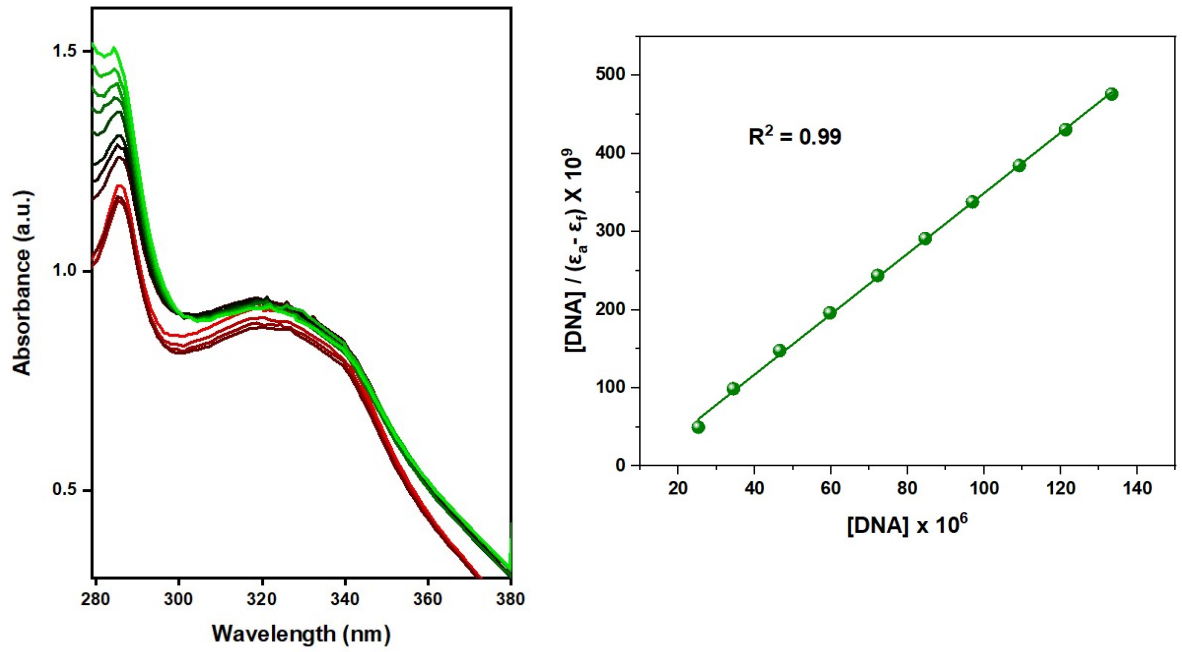

Figure S47. UV-Visible absorbance response of **L2** (1.0×10^{-5}) at pH 7.2 in 5 mM Tris-HCl-NaCl buffer solution in the presence of incremental addition of CT-DNA

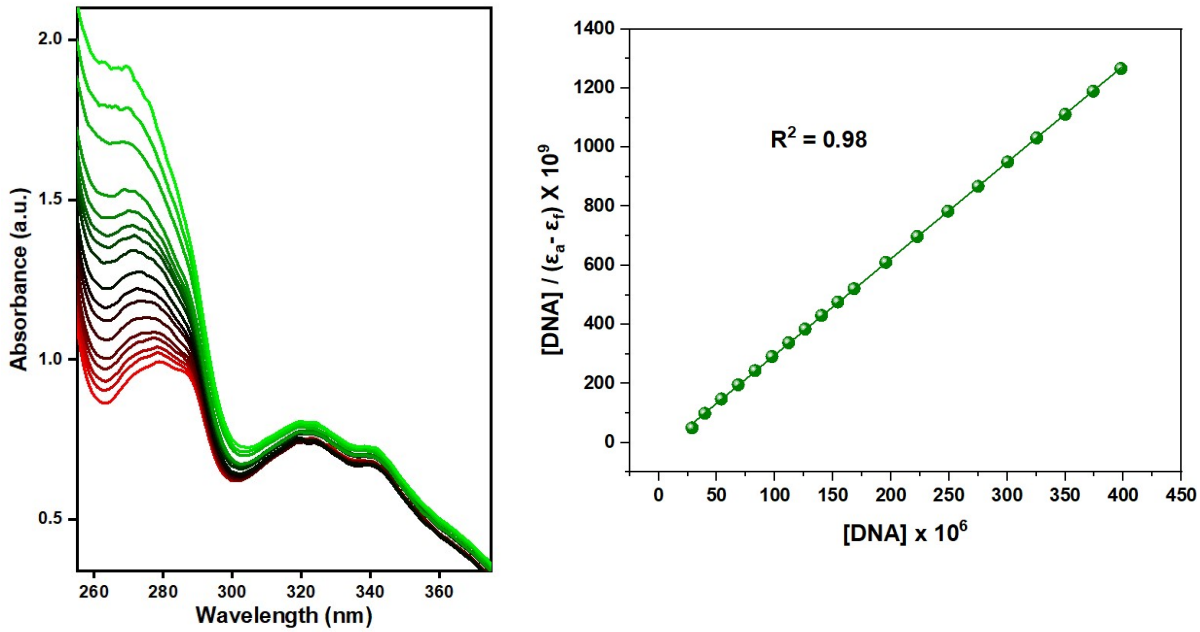

Figure S48. UV-Visible absorbance response of **NiL2** (1.0×10^{-5}) at pH 7.2 in 5 mM Tris-HCl-NaCl buffer solution in the presence of incremental addition of CT-DNA

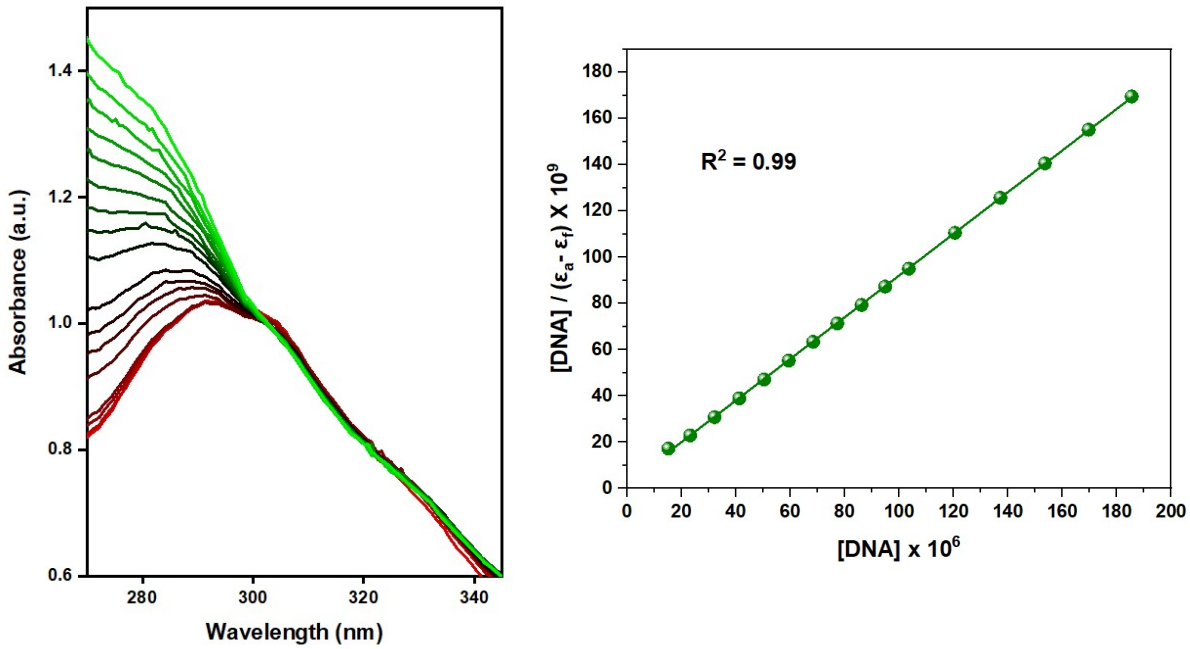

Figure S49. UV-Visible absorbance response of **L3** (1.0×10^{-5}) at pH 7.2 in 5 mM Tris-HCl-NaCl buffer solution in the presence of incremental addition of CT-DNA

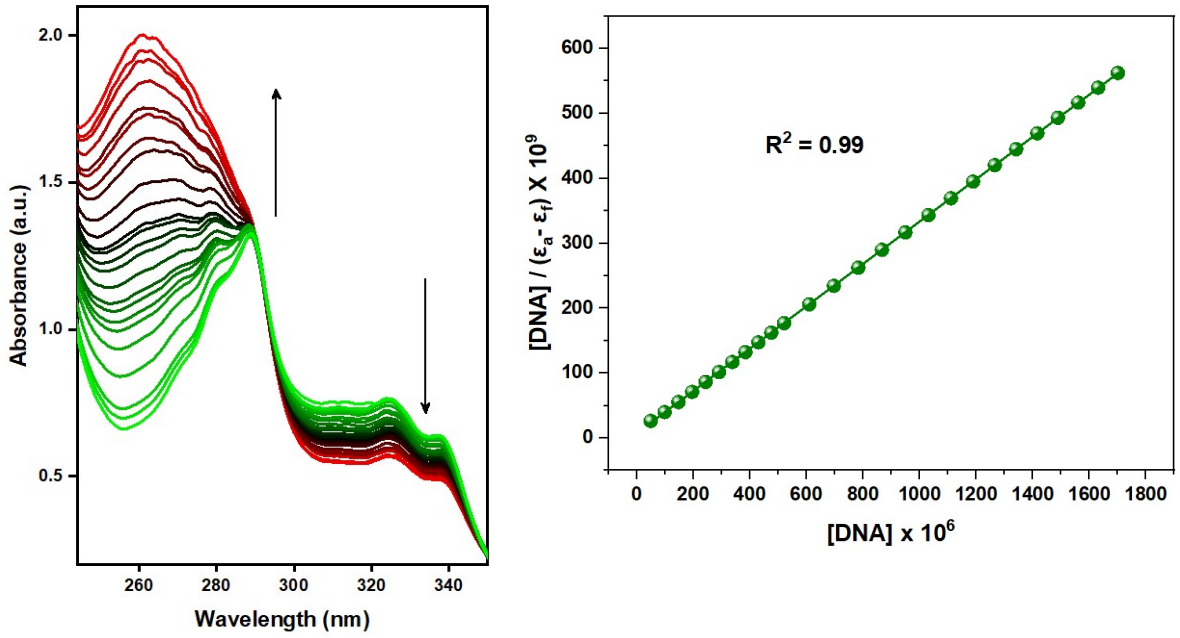

Figure S50. UV-Visible absorbance response of **NiL3** (1.0×10^{-5}) at pH 7.2 in 5 mM Tris-HCl-NaCl buffer solution in the presence of incremental addition of CT-DNA

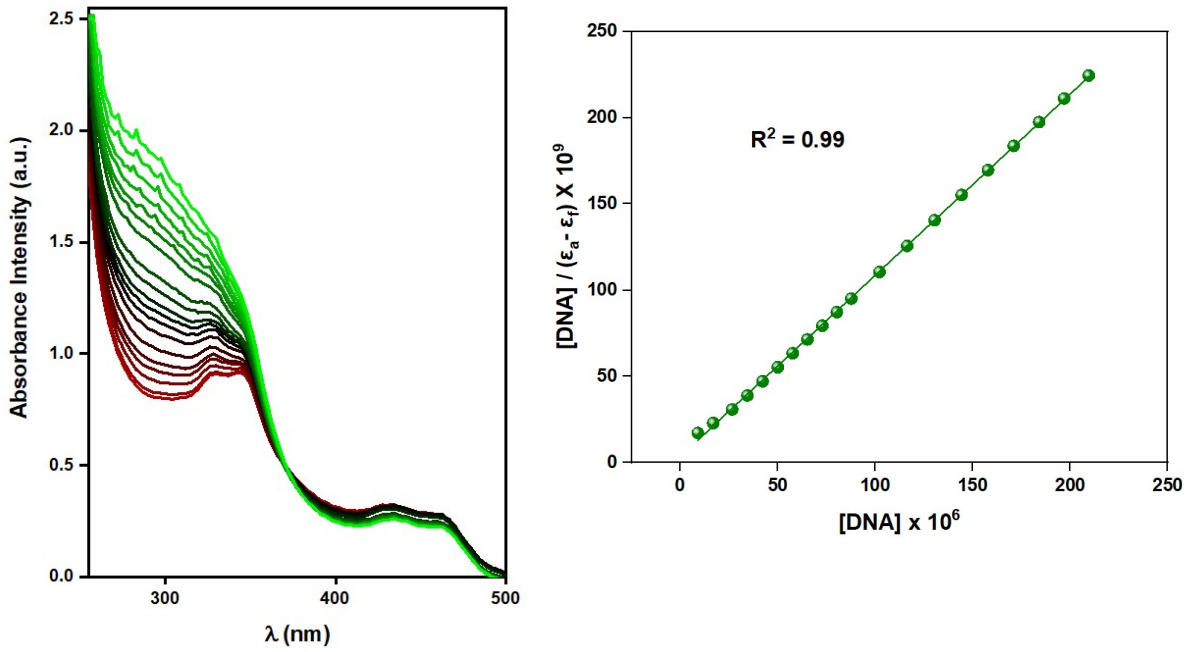

Figure S51. UV-Visible absorbance response of **L4** (1.0×10^{-5}) at pH 7.2 in 5 mM Tris-HCl-NaCl buffer solution in the presence of incremental addition of CT-DNA

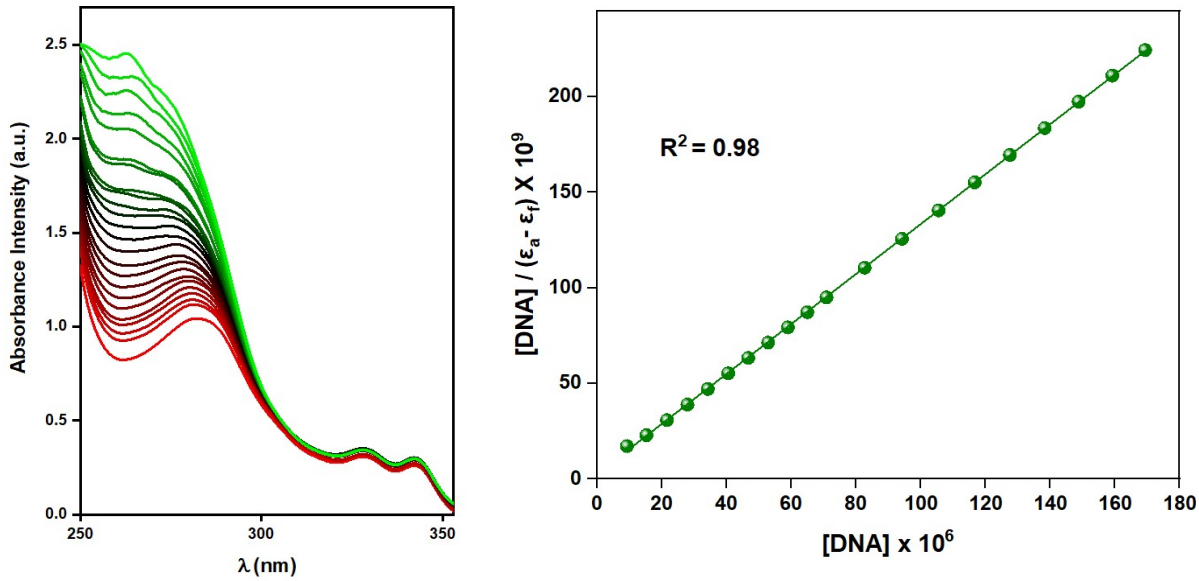

Figure S52. UV-Visible absorbance response of **NiL4** (1.0×10^{-5}) at pH 7.2 in 5 mM Tris-HCl-NaCl buffer solution in the presence of incremental addition of CT-DNA

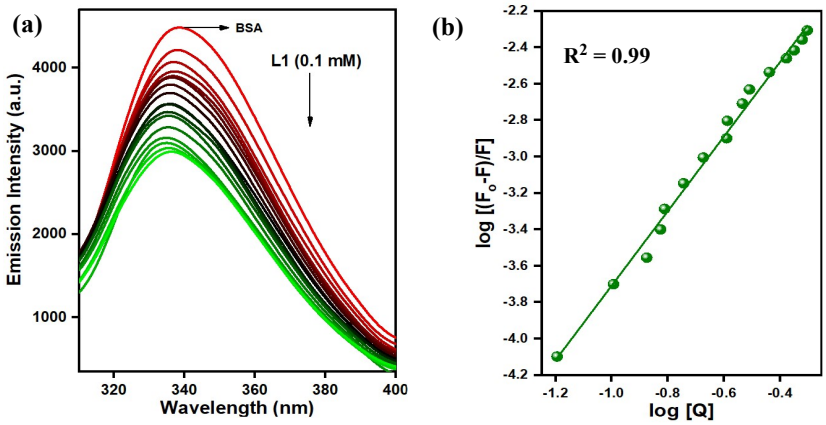

Figure S53 Binding parameters of interaction of the ligand (**L1**) with BSA

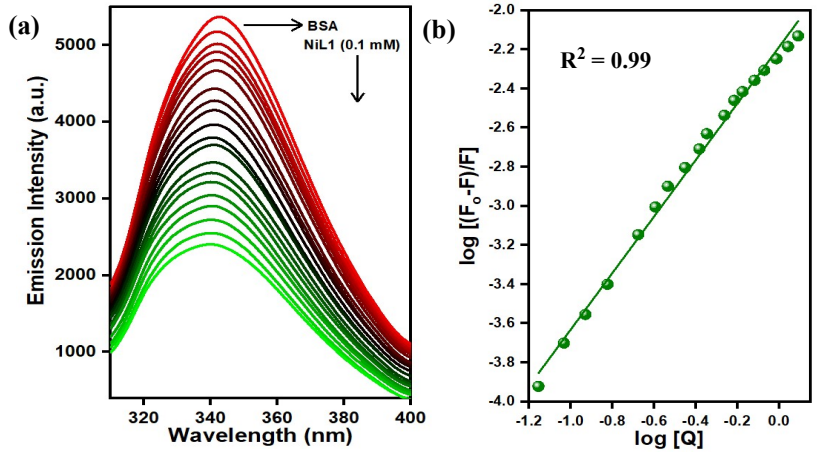

Figure S54 Binding parameters of interaction of the ligand (**NiL1**) with BSA

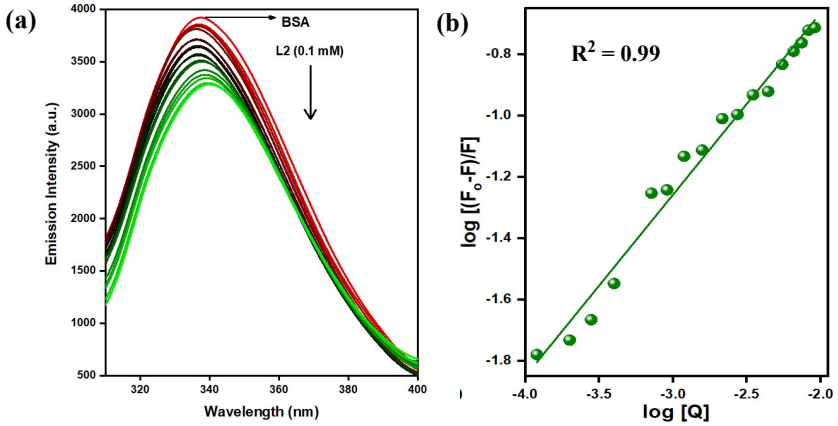

Figure S55 Binding parameters of interaction of the ligand (**L2**) with BSA

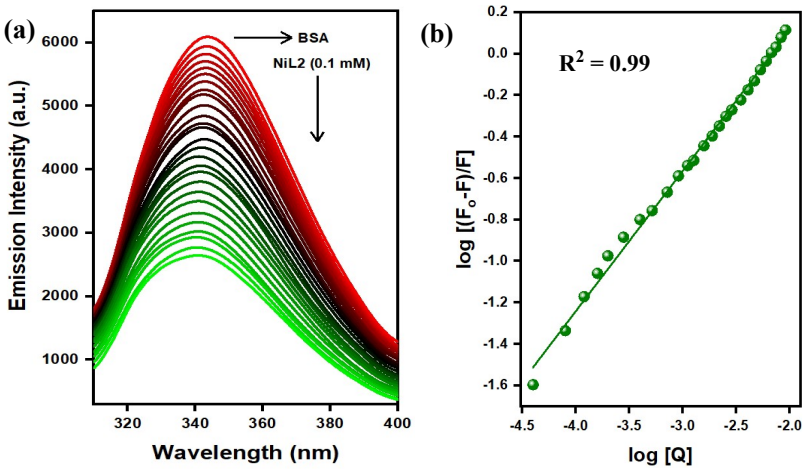

Figure S56 Binding parameters of interaction of the ligand (**NiL2**) with BSA

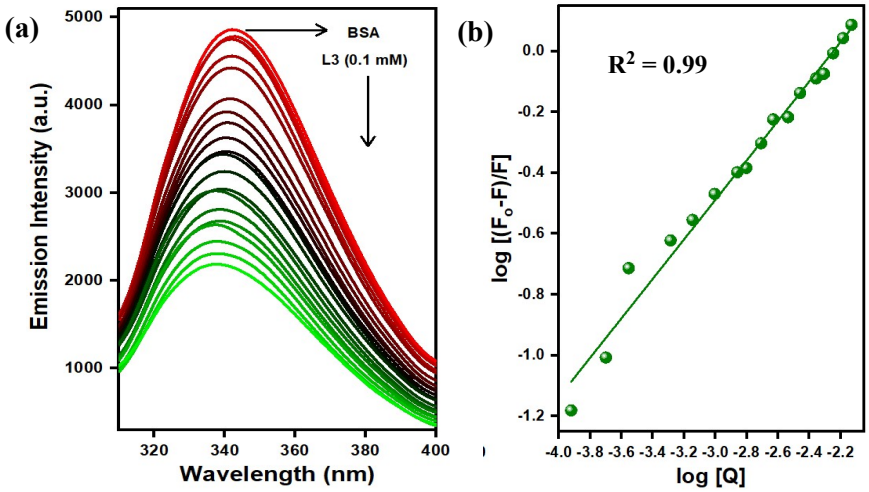

Figure S57 Binding parameters of interaction of the ligand (**L3**) with BSA

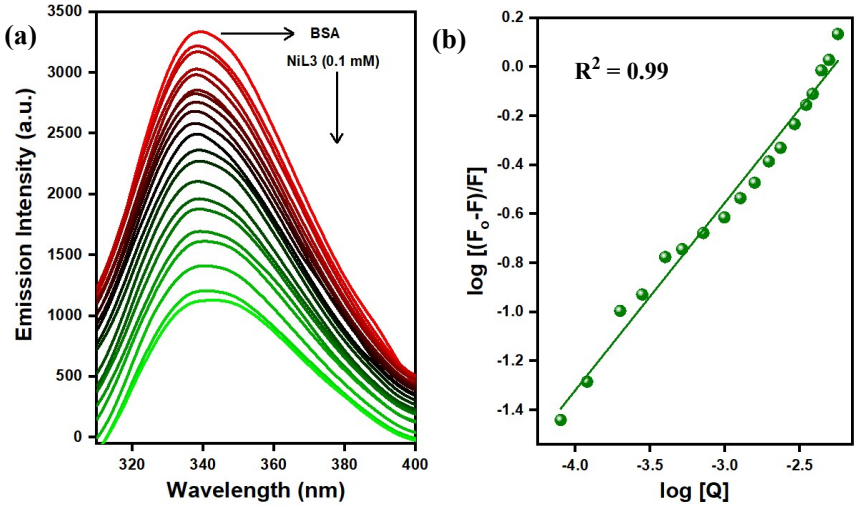

Figure S58 Binding parameters of interaction of the ligand (**NiL3**) with BSA

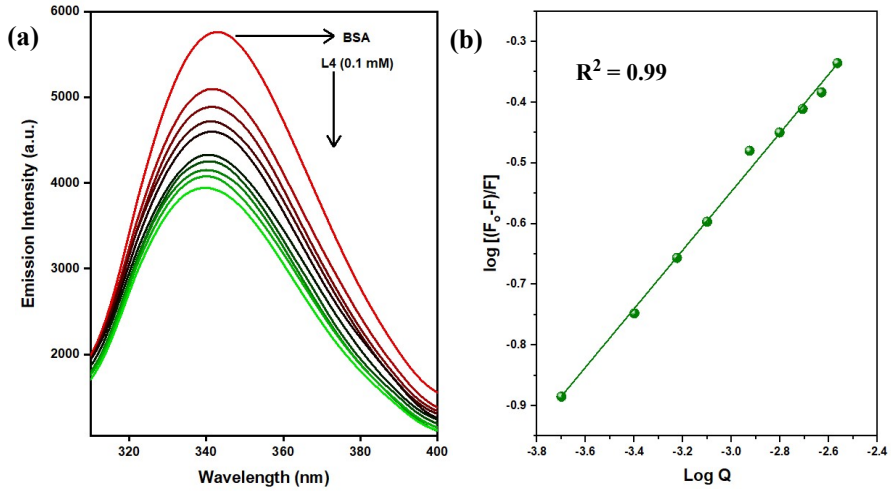

Figure S59 Binding parameters of interaction of the ligand (**L4**) with BSA

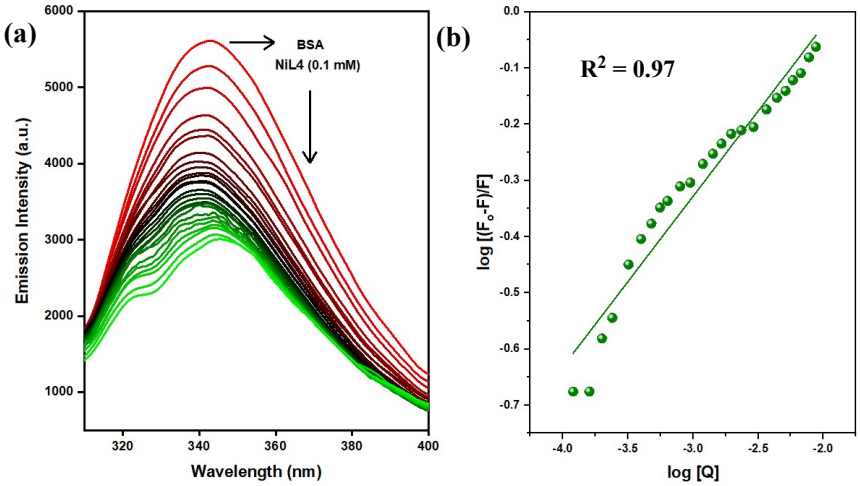

Figure S60 Binding parameters of interaction of the ligand (**NiL4**) with BSA

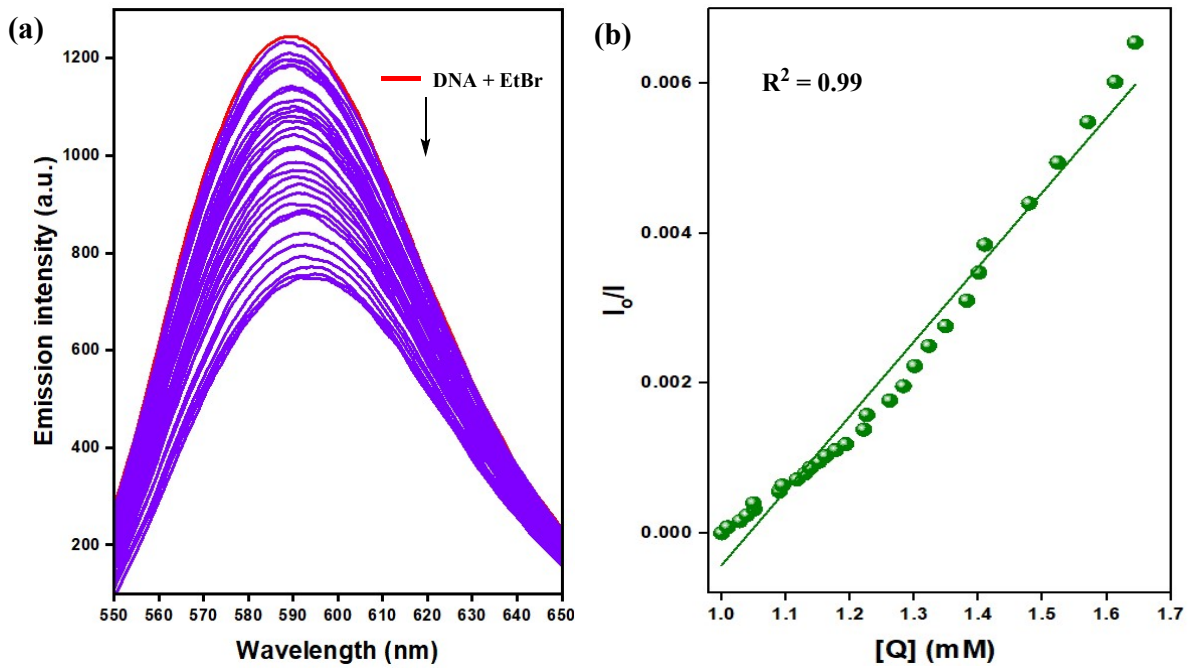

Figure S61 Fluorescence spectral response of the EtBr-DNA at pH 7.2 in the presence of **L1**

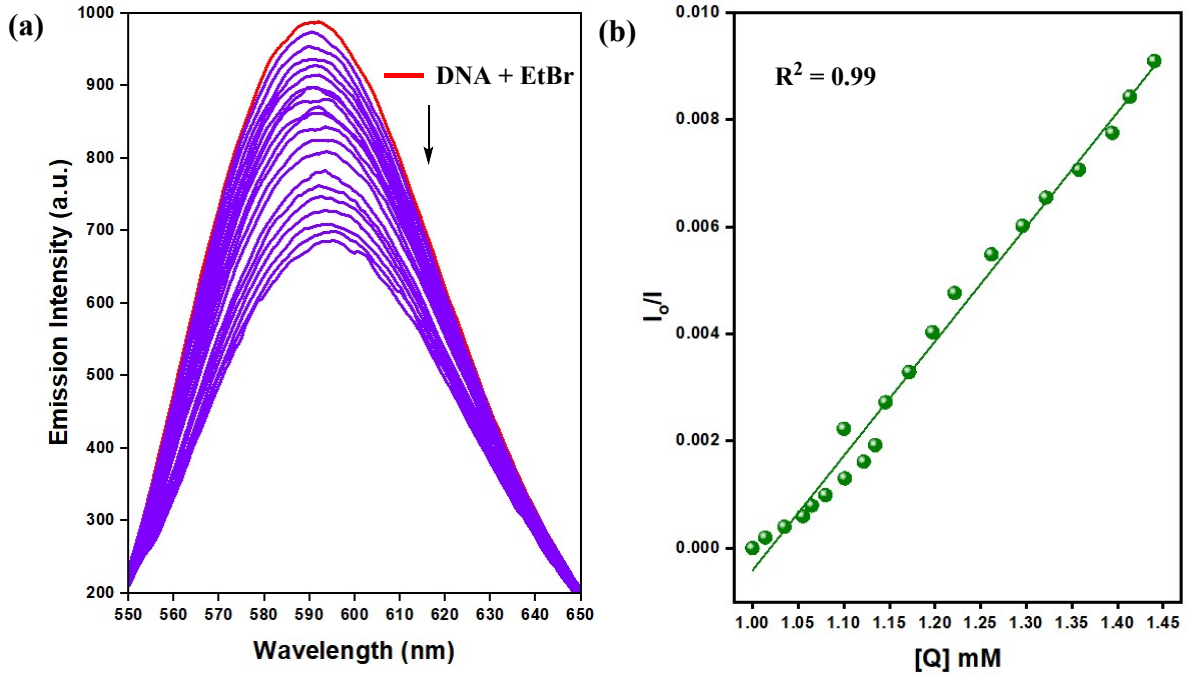

Figure S62 Fluorescence spectral response of the EtBr-DNA at pH 7.2 in the presence of **NiL1**

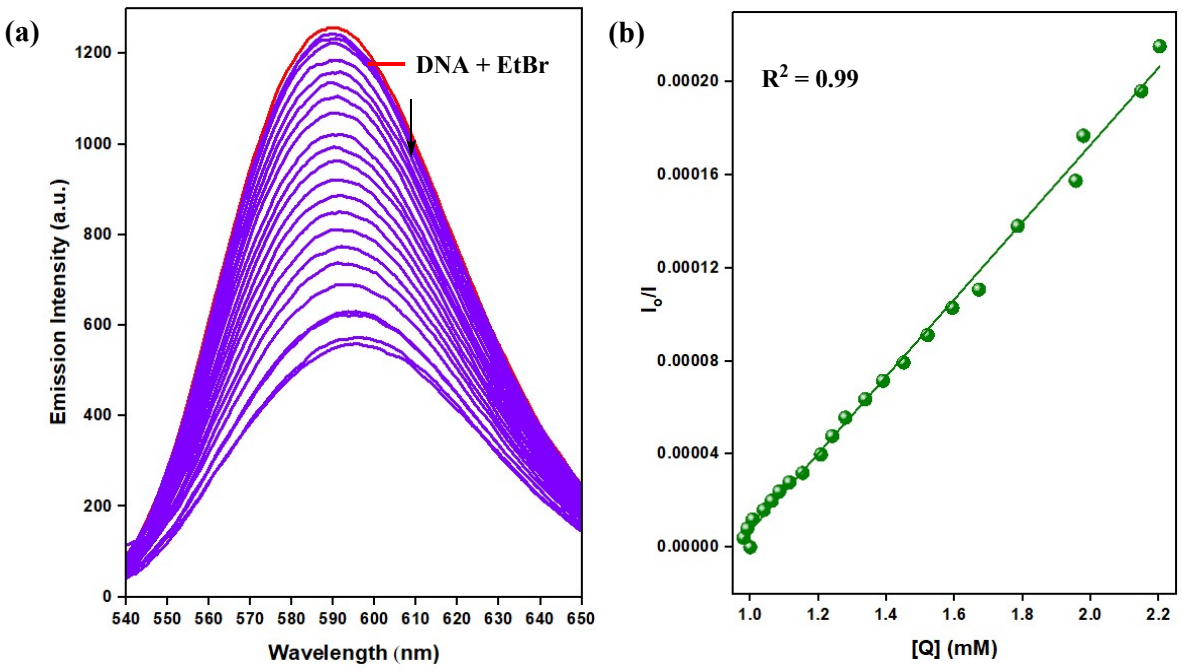

Figure S63 Fluorescence spectral response of the EtBr-DNA at pH 7.2 in the presence of **L2**

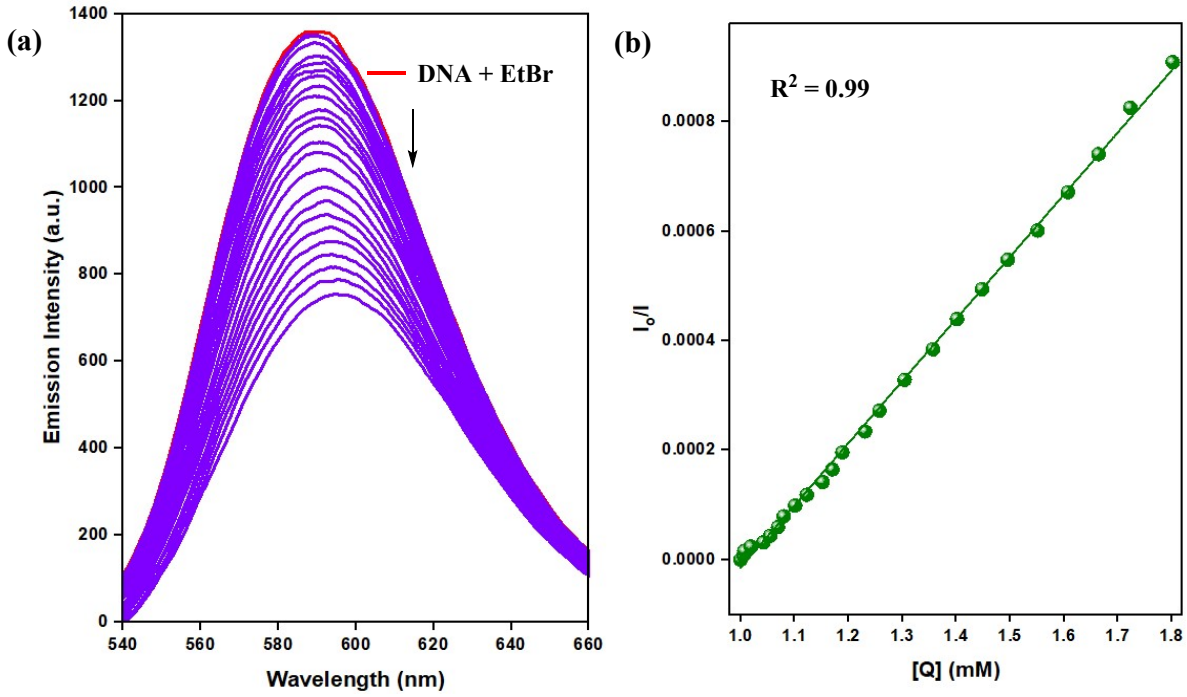

Figure S64 Fluorescence spectral response of the EtBr-DNA at pH 7.2 in the presence of **NiL2**

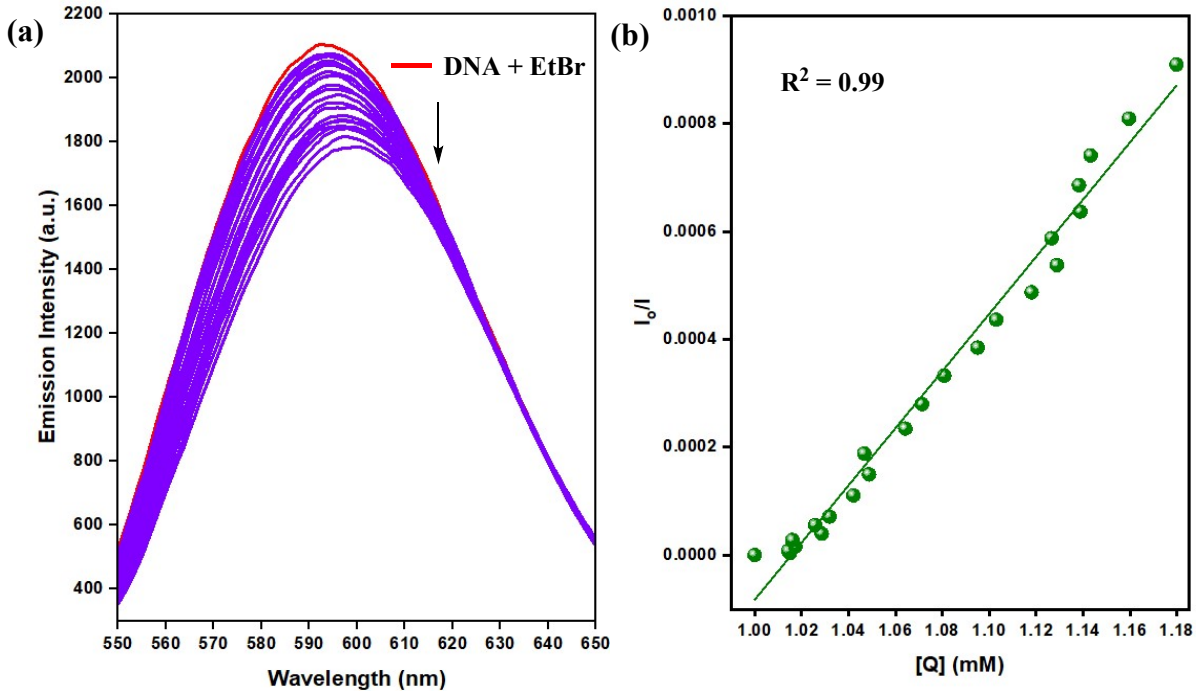

Figure S65 Fluorescence spectral response of the EtBr-DNA at pH 7.2 in the presence of **L3**

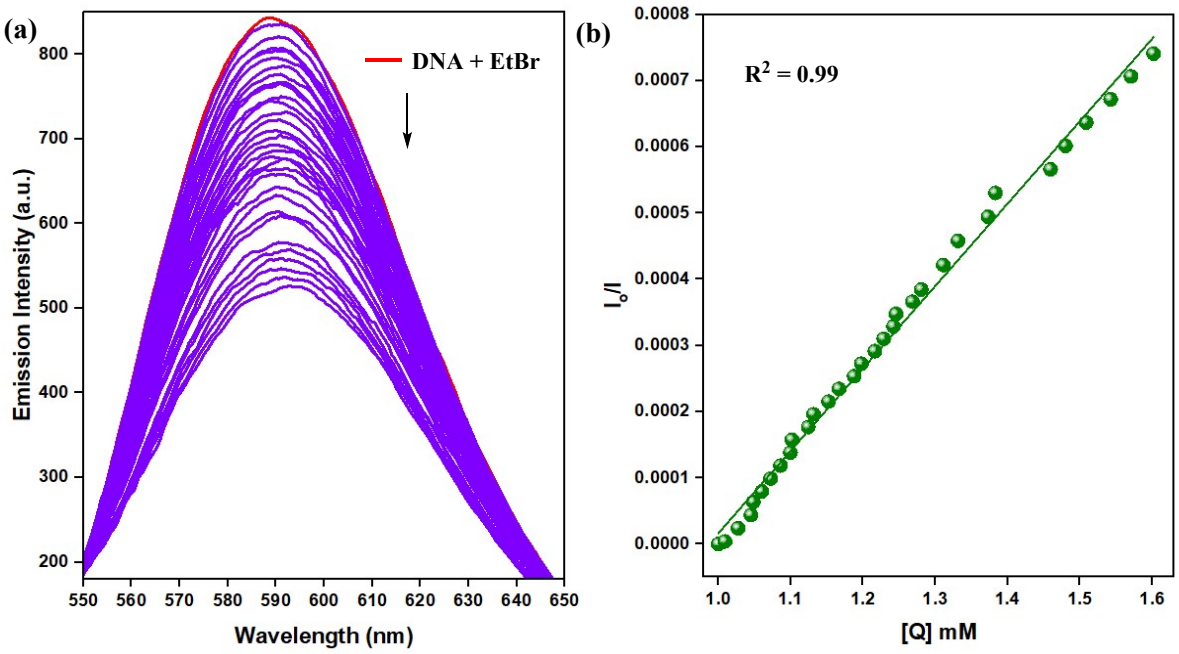

Figure S66 Fluorescence spectral response of the EtBr-DNA at pH 7.2 in the presence of **NiL3**

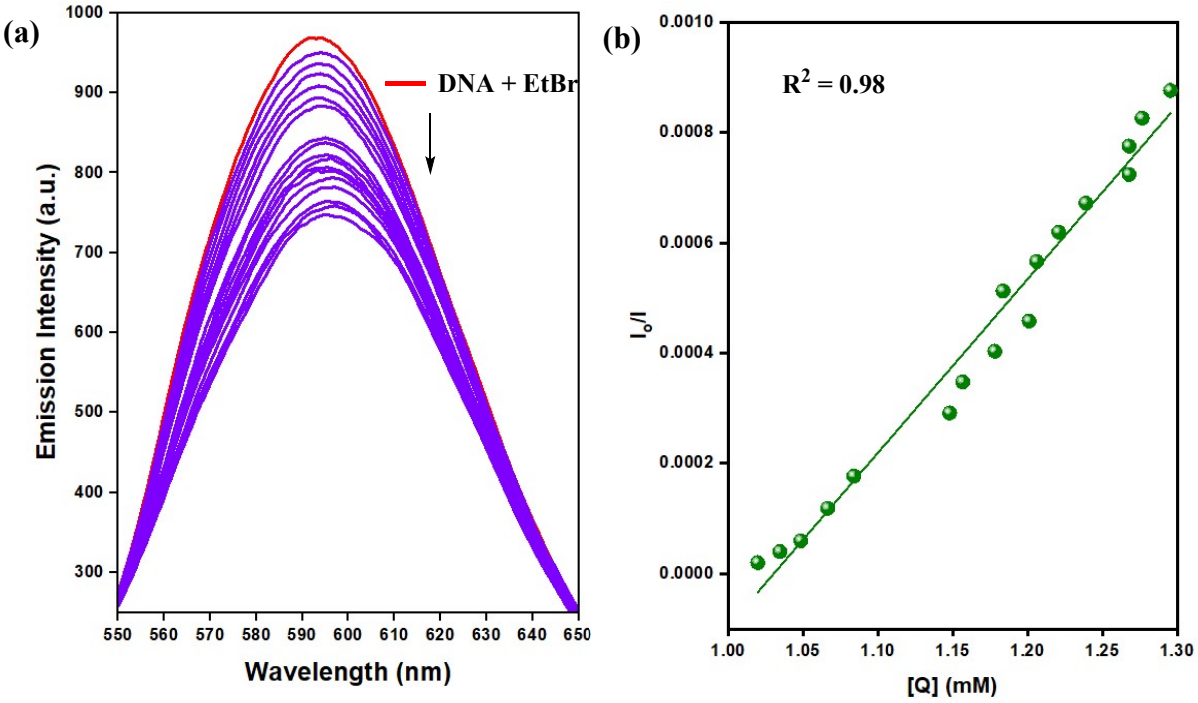

Figure S67 Fluorescence spectral response of the EtBr-DNA at pH 7.2 in the presence of **L4**

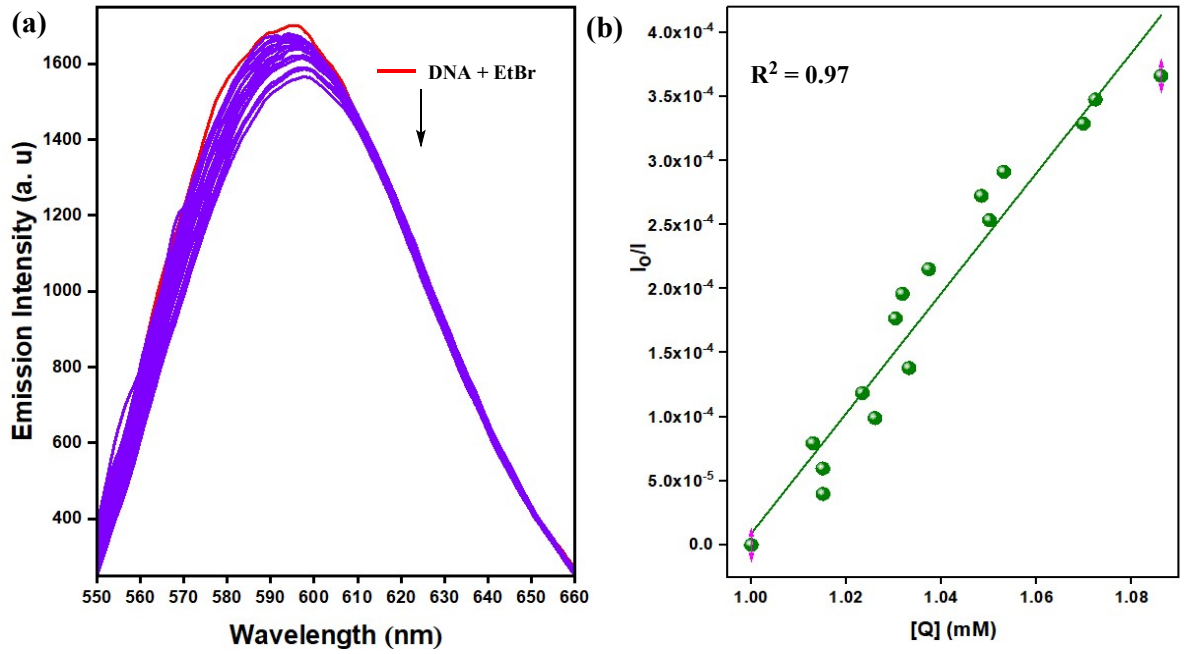

Figure S68 Fluorescence spectral response of the EtBr-DNA at pH 7.2 in the presence of **NiL4**

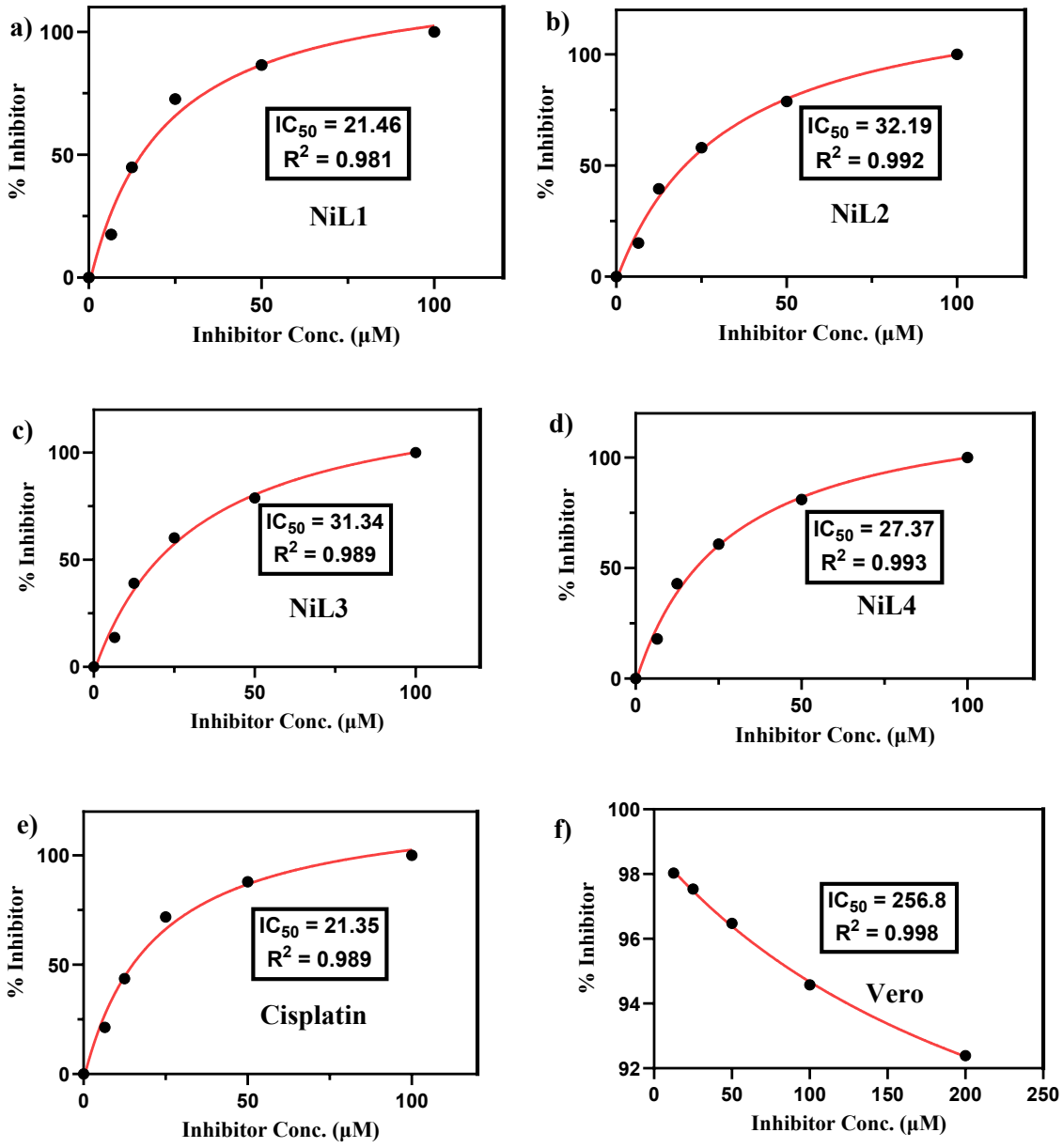

Figure S69. Sigmoidal plot for finding the IC_{50} Values of the Ni(II) complexes **NiL1-NiL4** (In order a-d) and using the standard drug Cisplatin (e) using Hep-G2 cell line. f) Sigmoidal plot for the Vero cell line.

Table S2. Crystallographic data refinement details of the ligand **L4** and the Ni(II) complex **NiL4**

Identification code	**L4**	**NiL4**
Empirical formula	$C_{26}H_{16}ClN_3O_2S$	$C_{28}H_{22}Cl_3N_3NiO_4S$
Formula weight (g/mol)	469.93	661.60
Temperature/K	300.00	300.00
Crystal system	Triclinic	Monoclinic
Space group	P-1	$P2_1/n$
a (Å)	8.238(2)	7.4934(11)
b (Å)	10.517(3)	26.809(4)
c (Å)	13.479(4)	14.499(2)
α (Å)	96.239(10)	90
β (Å)	102.378(10)	92.652(5)
γ (Å)	99.049(10)	90
Volume/ Å^3	1114.1(5)	2909.7(7)
Z	2	4
***P* (calc)g/cm^3**	1.401	1.510
θ for data collection	4.674 to 56.54	4.14 to 52.736
Reflections collected	49070	36563
Independent reflections	5464	5934
GOF on F^2	1.058	1.036
R1 [I>2σ]	0.0453	0.0551
wR2 [F^2]	0.0867	0.1193